Physica 100B (1980) 1–28
© North-Holland Publishing Company

COHESION IN ALLOYS – FUNDAMENTALS OF A SEMI-EMPIRICAL MODEL

A. R. MIEDEMA
Philips Research Laboratories, 5600 MD Eindhoven, The Netherlands

and

P. F. de CHÂTEL and F. R. de BOER
Natuurkundig Laboratorium, University of Amsterdam, 1018 XE Amsterdam, The Netherlands

Received 7 December 1979

A semi-empirical model of alloy cohesion involving two material constants for each element is introduced by means of the physical ideas underlying the scheme. The resulting expressions for the heat of formation of binary alloys are presented and their applicability in various extreme situations is discussed. The model is shown to reproduce a vast amount of experimental information on the sign of heats of formation. Detailed comparison with experiment for particular classes of alloys will be presented in the sequels to this paper.

1. Introduction

1.1. Types of cohesion

In simple treatments of binding in crystals, one attempts to classify solids according to the type of interaction holding them together. In some cases, e.g. molecular crystals or ionic compounds, the classification is relatively straightforward and easy to apply. The fact that a variety of electronegativity scales has been introduced to assess the relative importance of ionic binding shows that the delineation of this type from metallic and covalent binding is not easy. In fact, a similar ambiguity exists in the classification of metals and semiconductors, where the terms 'covalent' and 'metallic' are often applied to compounds in a rather suggestive way, without giving much insight into the origin of the cohesive energy.

In molecular crystals, which include the solid noble gases, one describes cohesion in terms of the Van der Waals – London interaction between molecules. The interaction being due to the mutually induced dipole moments of the two molecules, the cohesive energy depends quadratically on the molecular polarizability. There is no need for an overlap between the charge densities of the interacting molecules for this attractive force to be effective. In fact, the overlap provides the repulsive force that keeps the solid from collapsing. In the case of solid noble gases, we find a simple relation between the fairly small electron density between atoms and the cohesive energy at $T = 0$ per unit molar surface area (fig. 1). This correlation implies that there is a proportionality between negative and positive contributions to the total energy at the equilibrium interatomic distance.

In ionic crystals, the cohesive energy can be accounted for by electrostatic interactions between distinct, oppositely charged ions of well-defined sizes and charges. In the case of fully ionic substances, i.e., compounds containing ions of integral charge units, the calculation of the binding energy is a relatively simple matter. However, fully ionic compounds represent a limiting case, never actually realized in nature. Even in the textbook examples of ionic crystals (alkali halides, oxydes of metals with very low electronegativity) there must be some overlap between the oppositely charged ions which generates the necessary repulsive forces. Thus, one always deals with intermediate, partially ionic cases, where the electron density between ions is appreciable, and there is an ambiguity in the decomposition of the electronic charge distribution into positive and negative ions.

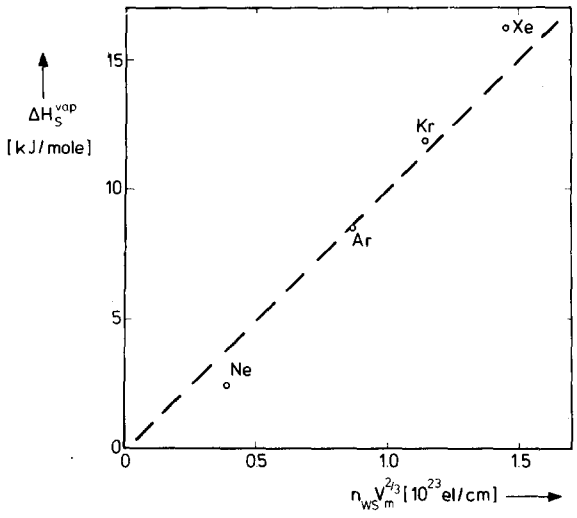

Fig. 1. Illustration of the approximate linear relationship between the cohesive energy per unit molar surface $\Delta H_s^{vap}/V_m^{2/3}$ (heat of vaporization at $T = 0$, corrected for zero-point motion [1]), of the noble gases and the averaged electron density, n_{WS}, at the boundary of the Wigner–Seitz cell. The values for n_{WS} have been obtained by summation of the electron densities of the free atoms [2] situated at the lattice positions at $T = 0$.

Metallic binding is said to be due to the delocalization of electrons, which leads to a lowering of their kinetic energy. More precisely, if one considers a single atomic orbital on each atom, superpositions of such states will constitute a band, comprising energies lower and higher than the atomic level. In metal formation there is a preferential occupation of those states that have lowered their energies. These are indeed the states with the lowest kinetic energy, having a vanishing slope of the wave function half-way between two atoms, in contrast to the highest states in the band, whose wave functions have maximum slope and zero value half-way between two atoms. The former states can be also termed bonding states, as opposed to the latter, antibonding states, since they deposit a maximum amount of negative charge between the positive ions. Apart from band broadening, energy is gained in metal formation through the admixture of higher atomic orbitals, which further lowers the energy of occupied states. As mutual dipole induction in the theory of Van der Waals–London interactions is also described by means of the admixture of higher, unoccupied states, this contribution to metallic binding is seen to be related to the binding mechanism in molecular crystals.

Covalent crystals are described in terms of bond charges resulting from the preferential occupation of bonding states, which we introduced above in connection with metallic binding. The distinction between metallic and covalent binding is sometimes rather artificial. If one insists on classifying silicon as a covalent crystal, one is implying that the cohesive energies in solid and liquid (metallic) silicon are of different origin. However, the energy lowering achieved by arranging Si atoms on the tetrahedral diamond lattice is of the order of the heat of fusion, which is only a small fraction of the cohesive energy. This suggests that, as far as cohesive properties are concerned, crystals of Si, Ge or grey Sn should be considered as metallic crystals in which the shape of the constant-energy surfaces and the number of electrons per atom are such that exactly one Jones zone is filled. It is then not surprising that such a strong deviation from a spherical Fermi surface is accompanied by a directional type of electron density distribution in real space. Naturally, the exact filling of the Jones zone cannot be considered an accident. The diamond structure with its two atoms per unit cell is favoured because of the possibility of separating bonding and antibonding states by an energy gap, and filling them up to the gap. However, such considerations are common in metal physics as well. They are involved, for instance, in the explanation of the Hume–Rothery rule, which establishes a correlation between the occurrence of ordered structures and particular values of the electron to atom ratio.

The above discussion is meant to make clear the inadequacy of the customary classification of solids, even for simple substances. When it comes to understanding alloys and intermetallic compounds, the situation becomes even more complicated. Adopting the principle that structure dependent energy contributions are due to covalent bonding, and recognizing that (as we hope to convincingly show in this and subsequent papers) the most important factor stabilizing an intermetallic compound of two transition metals with respect to its pure solid constituents is ionicity, one is forced to realize that discussions of alloy stability must take place on the ill-defined no man's land between three "pure" types of binding.

One can think of two ways out of this impasse, and

in both cases the first step is to discard the traditional classification. Then, either a new set of phenomenological concepts has to be introduced, or, more ambitiously, an exact theory has to be formulated and applied to various systems. Recent self-consistent energy-band and total-energy calculations [3] using the density functional formalism [4] have shown the feasibility of the latter approach. However, to perform such calculations for a large number of systems is not a practical proposal at the moment. Nor would one gain much insight from the resulting energies and charge distributions. To derive trends and regularities from these, one would again be faced with the problem that there is no unique way of decomposition. Therefore, we have undertaken the less ambitious approach of describing the heat of formation of alloys and intermetallic compounds in a new framework of concepts and empirical quantities. In the next subsection this framework will be sketched. Before formulating the problem of alloy formation in this framework, we will point out some analogies with a phenomenological treatment of the Van der Waals–London interactions. At the end of this section we discuss the relation of our scheme to earlier treatments of alloy formation.

1.2. The macroscopic atom picture

Admittedly, the remark made in the preceding section to the effect that the Van der Waals–London interaction and metallic binding have some common features was not very useful for the purpose of practical calculations. Surely, if one starts from isolated atoms, any energy lowering upon solidification can be described as a consequence of hybridization of states, but this observation does not make the problem of metallic cohesion as simple as that of the Van der Waals–London interactions. What makes the latter tractable is the fact that the admixture of higher states is so slight that perturbation theory is applicable. That this cannot be the case in metals can be simply deduced from the fact that here cohesive energies are more than an order of magnitude larger than for noble gas solids whereas the excited states of the free atoms lie lower. The fundamental nature of the difficulties in understanding metallic cohesion can be appreciated by considering that cohesive energies of metals are comparable to the corresponding typical atomic excitation energies, and amount to a substantial fraction of the ionization energies.

In problems of alloy stability, however, we are dealing only with formation energies, that is, differences between the cohesive energies of alloys and their constituents in the metallic state. What makes it difficult to make use of the fact that such energies are an order of magnitude smaller than cohesive energies, is that there is no obvious way to choose as reference systems, instead of free atoms, atoms as they are when imbedded in a metal. Our basic assumption will be that this can be done, and that many of the considerations that apply to the situation when two macroscopi pieces of metal are brought into contact remain valid for suitably defined "atoms in the metallic state".

In this "macroscopic atom picture", there is little difference between the interface energy between two blocks of metal and the heat of formation (heat of mixing) of intermetallic liquid alloys. Energy considerations are made in terms of contact interactions that take place at the interface between dissimilar atoms. This picture suggests a fundamental relationship between the surface energy of a solid or liquid and its heat of vaporization, which is also born out by the empirical data (fig. 2).

A new parameter of central importance in the description of interface phenomena on an atomic scale is the electron density parameter, n_{ws}. This is defined as the electron density at the boundary of the Wigner–Seitz cell (or more precisely, its average over the cell boundary) as derived for the pure elements in the metallic state. An alloy or intermetallic compound is thought to be built up of atomic cells, the electron density being kept unchanged as the cell is removed from the metal. When dissimilar cells are brought in contact in the alloy, there will be discontinuities in the electron density. Elimination of such discontinuities requires energy, hence a positive contribution to interface energies and heats of mixing or formation, determined by Δn_{ws}, can be expected. Since for metallic alloys or metal–metal interfaces it is but one contribution to the total formation energy, this energy is experimentally not accessible. However, it has been calculated theoretically by determining the total energies of the constituent metals in a constrained state having a suitably chosen atomic volume. More precisely, Alonso and Girifalco [8] have shown that these atomic volumes are uniquely determined by the

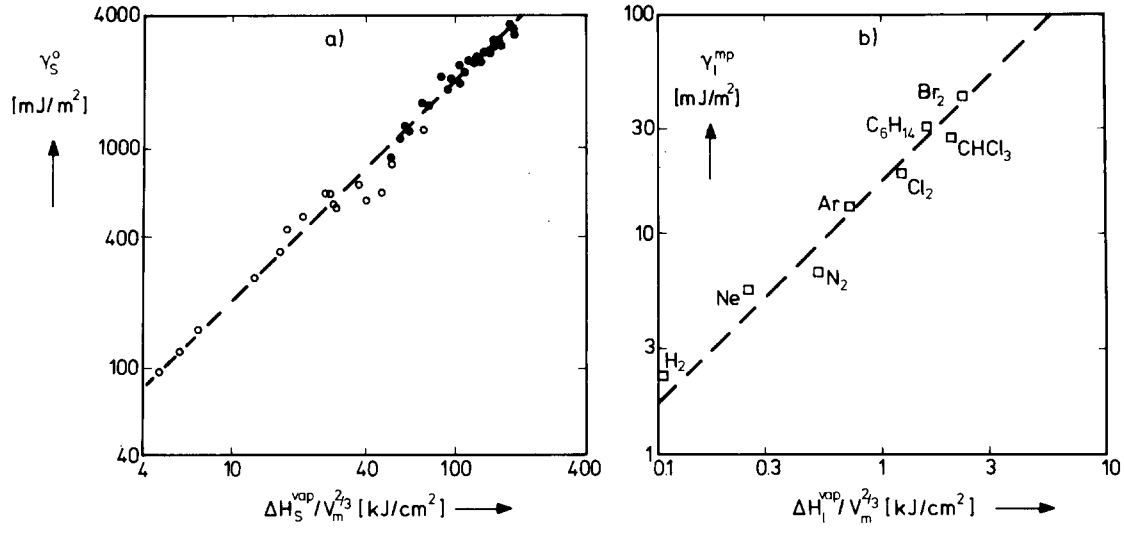

Fig. 2. Illustrations of the linear relationship between the heat of vaporization per unit molar surface, $\Delta H^{vap}/V_m^{2/3}$, and the surface energy γ.
(a) for solid metals at $T = 0$. Open circles correspond to non-transition metals, filled circles to transition metals. The divalent metals Be, Mg, Zn, Cd and Hg have been omitted. They are exceptional because of the unusual stability of the free atom s^2 outer electron configuration which is lost upon formation of the solid metal. This extra stability amounts to about 100–150 kJ/mole, which should be added to the experimental heats of vaporization of the divalent metals to make them comparable to the heats of vaporization of the other metals (see ref. 5 for further details). Data on γ_s^0 have been taken from ref. 6, see table I. The proportionality constant between γ_s^0 and $\Delta H_s^{vap}/V_m^{2/3}$ equals 2×10^{-9}.
(b) for Van der Waals liquids at their melting temperature [7] (γ_s^0 is not available). The proportionality constant equals 1.6×10^{-9}

requirement that their concentration-weighted average give the volume per atom in the alloy and that n_{ws} be the same for the two metals. The elastic energy calculated by Alonso and Girifalco agrees in approximate magnitude with the positive term introduced in the macroscopic atom approach. Recently, Williams et al. [9] have criticized the interpretation of the density mismatch energy in terms of elastic energies on the ground of first-principles band structure and total energy calculations. The existence of the density-mismatch term is born out by these calculations, but the results suggest that it corresponds to changes in the relative contributions of s, p, and d states to the total charge density, rather than to elastic energies. In a transition metal, an increase in n_{ws} can be realized by increasing the s-type and reducing the d-type contribution.

The empirical evidence for the existence of an electron-density mismatch term is not limited to alloy formation energies. Fig. 3 shows that there is an approximate linear relation between the surface energy of a metal and n_{ws}. The relevance of the electron density parameter to metallic cohesion is born out by fig. 4, which shows a linear relation, implied by figs. 2 and 3, between the heat of vaporization per unit atomic surface and n_{ws}. The similarity between figs. 1 and 4 is somewhat misleading: the slopes of the two straight-line fits are different by a factor of four. However, the analogy is sufficiently encouraging to study the problem of miscibility of Van der Waals liquids in the hope of learning something about alloying behaviour of metals.

1.3. Hildebrand's solubility parameter

The interaction energy between two non-polar molecules is proportional to the polarizability, P, of both molecules. Therefore, the cohesive energy of the condensed phase is proportional to P^2, and so is γ^0, the surface energy at $T = 0$. Applying the argument to macroscopic bodies, it is easily shown that the adhesive energy between two layers of Van der Waals

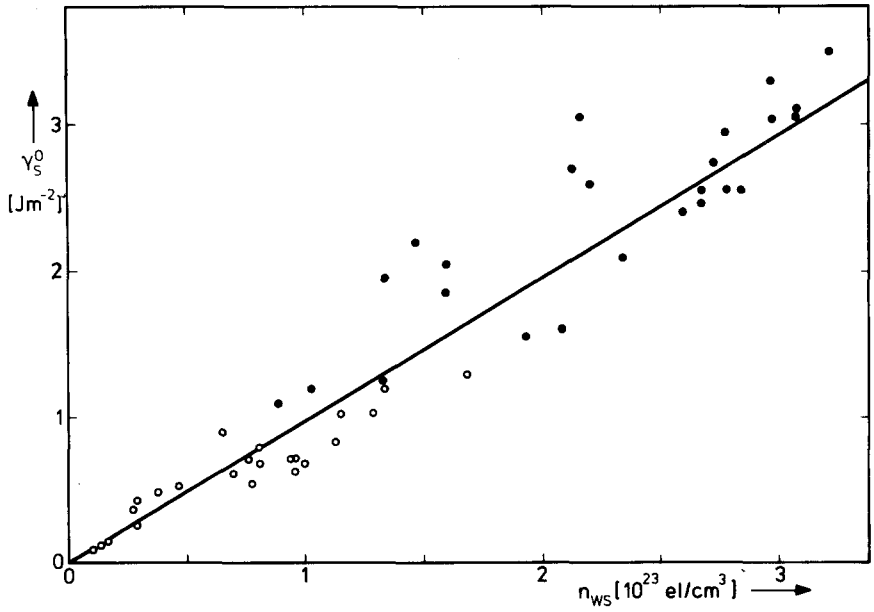

Fig. 3. The approximate linear relationship between the surface energy at $T = 0$, γ_s^0, and the interatomic electron density, n_{ws}, for non-transition metals (open circles) and transition metals (filled circles). For the non-transition metals the values for n_{ws} have been obtained by summation of the electron densities of the free atoms [2]. For the transition metals the n_{ws} values were derived from bulk modulus data [10]. The deviations from linearity have some systematics, which have been explained in ref. 6.

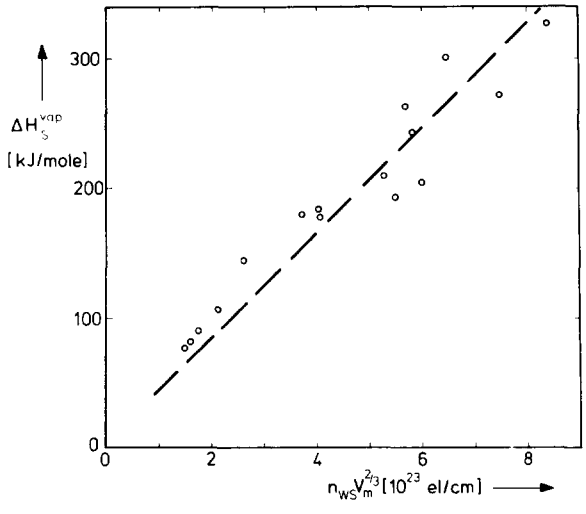

Fig. 4. The linear relation, implied by figs. 2 and 3, between the heat of vaporization per unit atomic surface, $\Delta H_s^{vap}/V_m^{2/3}$, and the electron density, n_{ws}, for non-transition metals. In this figure the divalent metals with their unusually low heat of vaporization have been omitted.

substances A and B in contact is proportional to $P_A P_B$, and equals $-2(\gamma_A^0)^{1/2}(\gamma_B^0)^{1/2}$ per unit surface area. The interface energy between two non-mixing Van der Waals liquids is then

$$\gamma_{AB}^0 = \gamma_A^0 + \gamma_B^0 - 2(\gamma_A^0)^{1/2}(\gamma_B^0)^{1/2}$$
$$= [(\gamma_A^0)^{1/2} - (\gamma_B^0)^{1/2}]^2. \quad (1)$$

The same result should apply to interfaces between Van der Waals solids, provided there is perfect matching, that is, no positive energy contribution due to elastic deformations.

If we apply this result to "interfaces" on an atomic scale, and make use of the linear relationship between γ^0 and the heat of vaporization per unit molar surface (cf. fig. 2), we find the enthalpy of solution of, say, liquid B in liquid A as

$$\Delta H_{B \text{ in } A}^{sol} = V_B^{2/3}\left[\left(\frac{\Delta H_A^{vap}}{V_A^{2/3}}\right)^{1/2} - \left(\frac{\Delta H_B^{vap}}{V_B^{2/3}}\right)^{1/2}\right]^2. \quad (2)$$

This is very similar to Hildebrand's formula for the mutual heat of solution of non-electrolyte liquids [11]:

$$\Delta H^{\text{sol}}_{\text{B in A}} = V_{\text{B}}\left[\left(\frac{\Delta H^{\text{vap}}_{\text{A}}}{V_{\text{A}}}\right)^{1/2} - \left(\frac{\Delta H^{\text{vap}}_{\text{B}}}{V_{\text{B}}}\right)^{1/2}\right]^2, \quad (3)$$

where $\Delta H^{\text{vap}}/V$ is the so-called solubility parameter. As was noted already by Hildebrand, considerations based on the macroscopic-atom picture lead to a slightly different definition of the solubility parameter, involving the 2/3 power of the molar volume. However, for liquids of comparable molar values, the two definitions are equivalent, as far as the prediction of heats of mixing is concerned.

At this point, we should note that Hildebrand's solubility parameter has been found to be a quantity of great practical importance. Predictions regarding the miscibility or immiscibility of Van der Waals liquids, based on the solubility parameter, are highly accurate. Enthalpies of mixing can be calculated by attaching a simple factor $f(c) = c^V_{\text{A}} \cdot c^V_{\text{B}}$, accounting for the concentration dependence, to expression (3) (the c^V's are volume concentrations). Equally satisfactory results can be obtained from eq. (2), if the multiplicative factor is chosen as $f(c) = c^{\text{s}}_{\text{A}} \cdot c^{\text{s}}_{\text{B}}$, where c^{s} stands for surface concentration.

We are inclined to consider the solubility parameters involving the molar surface area and the corresponding surface concentrations in mixtures to be the more fundamental set of parameters. The preference to use $(\Delta H^{\text{vap}}/V)^{1/2}$ in predictions of heats of mixing prevails mainly for historical reasons. Yet, the alternative treatment in terms of surface energies is not new. Langmuir [12] used this approach already sixty years ago in his description of heats of mixing in solutions of polar molecules.

Eqs. (1) and (2) can be rewritten in terms of the discontinuity in the electron density at the contact surface between different substances. Using the linear relationship between $\Delta H^{\text{vap}}/V^{2/3}$ and n_{ws} (fig. 1) we find

$$\Delta H^{\text{sol}}_{\text{B in A}} = Q' V_{\text{B}}^{2/3} \left[(n^{\text{A}}_{\text{ws}})^{1/2} - (n^{\text{B}}_{\text{ws}})^{1/2}\right]^2, \quad (4)$$

where Q' is a constant to be determined empirically.

1.4. Heat effects on alloying

It is clear that the results of the preceding section cannot be applied directly to alloys. The existence of stable alloys and intermetallic compounds indicates that eq. (4) does not give a full account of alloy formation. Having found that n_{ws} is just as important a parameter in metal cohesion as in the binding and mixing of Van der Waals substances, we may expect that a density-mismatch term like (4) will appear in a general expression of alloy formation energies. Whereas for Van der Waals substances this positive term is the only one that shows up in the heat of mixing of liquids, for metallic alloys there must be an additional, negative term.

We can understand the physical background of the negative term, if we try to reconstruct the arguments leading to eq. (4) with metallic interfaces in mind. When two blocks of different metals are brought in contact, the charge redistribution will not be limited to the inside of each block, but there will be a net charge transfer, governed by the difference in contact potential between the two metals. Charge will flow to places of lower potential energy, until the resulting dipole layer compensates the potential difference. Visualized on an atomic scale, this charge transfer corresponds to a negative, ionic contribution to the heat of formation.

In order to describe ionicity in metals, we have introduced [10, 13–15] the parameter ϕ^*. In the true spirit of the macroscopic atom picture, we should use ϕ, the work function of the pure metallic elements, when discussing interfaces between dissimilar atoms. The asterisk in ϕ^* will remind us that the work function had to be readjusted, by amounts comparable to the experimental uncertainty of ϕ values, in order to arrive at a set of parameters relevant to alloying behaviour (see table I). The form of the negative energy term involving ϕ^* reflects, however, its origin as a dipole-layer energy:

$$\Delta H^{\text{dip}}_{\text{AB}} = -P' S(\phi^*_{\text{A}} - \phi^*_{\text{B}})^2/(n^{-1/3}_{\text{ws}})_{\text{av}}, \quad (5)$$

where S is the contact surface area; P' is a constant to be determined empirically, that contains the electronic charge; the average value of $n^{-1/3}_{\text{ws}}$ enters the expression as a measure of electrostatic screening length, which determines the width of the dipole layer.

Table Ia

Metal	ϕ^* (V) [10, 13–15]	$n_{ws}^{1/3}$ $((d.u.)^{1/3})$ [10, 13–15]	$V_m^{2/3}$ (cm^2)	γ_s^0 (mJ/m^2) [6]	BV_m (kJ/mole) [26]
Sc	3.25	1.27	6.1	1200	6.6
Ti	3.65	1.47	4.8	2050	11
V	4.25	1.64	4.1	2600	14
Cr	4.65	1.73	3.7	2400	14
Mn	4.45	1.61	3.8	1600	4.4
Fe	4.93	1.77	3.7	2550	12
Co	5.10	1.75	3.5	2550	13
Ni	5.20	1.75	3.5	2450	12
Y	3.20	1.21	7.3	1100	7.2
Zr	3.40	1.39	5.8	1950	12
Nb	4.00	1.62	4.9	2700	18
Mo	4.65	1.77	4.4	2950	26
Tc	5.30	1.81	4.2	3050	26
Ru	5.40	1.83	4.1	3050	26
Rh	5.40	1.76	4.1	2750	23
Pd	5.45	1.67	4.3	2100	16
La	3.05	1.09	8.0	900	5.5
Hf	3.55	1.43	5.6	2200	15
Ta	4.05	1.63	4.9	3050	22
W	4.80	1.81	4.5	3300	31
Re	5.40	1.86	4.3	3650	33
Os	5.40	1.85	4.2	3500	35
Ir	5.55	1.83	4.2	3100	25
Pt	5.65	1.78	4.4	2550	18
Th	3.30	1.28	7.3[a]		
U	4.05	1.56	5.6[a]		
Pu	3.80	1.44	5.2[a]		
Cu	4.55	1.47	3.7	1850	9.3
Ag	4.45	1.39	4.7	1250	10
Au	5.15	1.57	4.7	1550	18

[a]Room temperature allotrope.

Combining eqs. (4) and (5), we can write for the heat of solution of metal B in metal A

$$\Delta H^{sol}_{B \text{ in } A} = - P V_B^{2/3} (\Delta\phi^*)^2 / (n_{ws}^{-1/3})_{av} + Q' V_B^{2/3} (\Delta n_{ws}^{1/2})^2. \quad (6)$$

For the relatively small differences in n_{ws} that occur between metals, one can combine the two terms of eq. (6) in the almost equivalent form

$$\Delta H^{sol}_{B \text{ in } A} = P \frac{V_B^{2/3}}{(n_{ws}^{-1/3})_{av}} \times \left\{ - (\Delta\phi^*)^2 + \frac{Q}{P} (\Delta n_{ws}^{1/3})^2 \right\}, \quad (7)$$

which contains, in brackets, our key expression for the heat of formation of binary alloys. Like eq. (1), this relation is only expected to hold, if there is no significant elastic energy due to size mismatch. Presumably, such size mismatch terms do not arise in liquids, and eq. (7) should give good results for the enthalpies of solution of liquid metals. To obtain the enthalpy of mixing, the prefactor has to be replaced by another one, involving surface concentrations (see eq. (9) below). Another class of materials where elastic size mismatch terms are not expected to play an important role is constituted by intermetallic compounds. If the negative, electronegativity term exceeds the positive one, such compounds will form at those concentrations at which a structure exists that can accommodate the

Table Ib

Metal	ϕ^* (V) [10, 13–15]	$n_{ws}^{1/3}$ $((d.u.)^{1/3})$ [10, 13–15]	$V_m^{2/3}$ (cm^2)	γ_s^0 (mJ/m^2) [6]	BV_m (kJ/mole) [26]
Li	2.85	0.98	5.5	530	1.5
Na	2.70	0.82	8.3	260	1.6
K	2.25	0.65	12.8	150	1.5
Rb	2.10	0.60	14.6	120	1.8
Cs	1.95	0.55	16.8	95	1.4
Ca	2.55	0.91	8.8	490	4.0
Sr	2.40	0.84	10.2	430	3.9
Ba	2.32	0.81	11.3	370	3.9
Be	4.20	1.60	2.9	(1900)	4.9
Mg	3.45	1.17	5.8	790	5.0
Zn	4.10	1.32	4.4	1020	5.5
Cd	4.05	1.24	5.5	780	6.1
Hg	4.20	1.24	5.8	610	4.0
B	4.75	1.55	2.8		
Al	4.20	1.39	4.6	1200	7.2
Ga	4.10	1.31	5.2	830	6.7
In	3.90	1.17	6.3	690	6.4
Tl	3.90	1.12	6.6	610	6.2
C	6.20	1.90	1.8		
Si	4.70	1.50	4.2[a]	1290[a]	11.9
Ge	4.55	1.37	4.6[a]	1030[a]	10.5
Sn	4.15	1.24	6.4	710	8.8
Pb	4.10	1.15	6.9	610	7.9
N	7.00	1.60	2.2		
As	4.80	1.44	5.2[a]	1000[a]	5.1
Sb	4.40	1.26	6.6[a]	680[a]	7.0
Bi	4.15	1.16	7.2[a]	550[a]	6.7

[a]For Si, Ge, As, Sb and Bi we have introduced hypothetical metallic allotropes corresponding to the properties of these elements in metallic systems.

constituent atoms without generating an elastic mismatch energy.

A consequence of the simple structure of eq. (7) is that, provided Q and P are truly constant for arbitrary choices of metals A and B, the sign of the heat of alloy formation is simply determined by the ratio $\Delta\phi^*/\Delta n_{ws}^{1/3}$: for $(\Delta\phi^*/\Delta n_{ws}^{1/3})^2 > Q/P$ the heat of formation is negative, if the opposite inequality holds, it is positive. The reliability of eq. (7) in predicting the sign of the heat of mixing of liquid alloys is demonstrated in fig. 5 for liquid binary systems involving two non-transition metals. Each symbol in the $|\Delta\phi^*|$ vs $|\Delta n_{ws}^{1/3}|$ diagram corresponds to a binary system; a negative sign meaning $\Delta H^{mix} < -2.5$ kJ/mole of alloys of the equiatomic composition, and, similarly, a positive sign corresponding to $\Delta H^{mix} > +2.5$ kJ/mole. It is seen that, with the ϕ^* and $n_{ws}^{1/3}$ values listed in table I, eq. (7) gives a good approximation to ΔH^{mix}: omitting systems with $|\Delta H^{mix}| < 2.5$ kJ/mole, we get an almost perfect separation between + and − signs by drawing a straight line in the $\Delta\phi^*$, $\Delta n_{ws}^{1/3}$ map. Fig. 6 shows that although relaxing the restriction $|\Delta H^{mix}| > 2.5$ kJ/mole spoils the almost perfect separation, the sign of the heat of mixing is quite accurately predicted even if the total energy effect is small. In fig. 7, similar information is compiled for liquid alloys of transition or noble metals in combination with transition, noble, alkali, or alkaline-earth metals (the common feature of these groups is that there is very little p-character in the wave functions of their conduction electrons). It is important to note that the slope of the straight line separating + from −

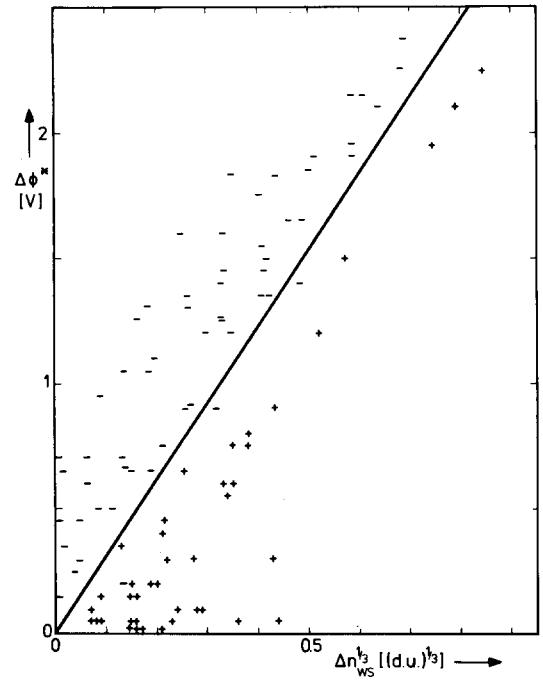

Fig. 5. Demonstration of the reliability of eq. (7) in predicting the sign of the heat of mixing of liquid alloys not containing transition or noble metals. Each symbol corresponds to one binary system. The meanings of the signs are: −: $\Delta H^{\text{mix}} < -2.5$ kJ/mole of atoms of the equiatomic composition; +: $\Delta H^{\text{mix}} > +2.5$ kJ/mole of atoms of the equiatomic composition, or the liquid system has a central miscibility gap, or the solubility of at least one of the metals is very small at temperatures above 1000 K.

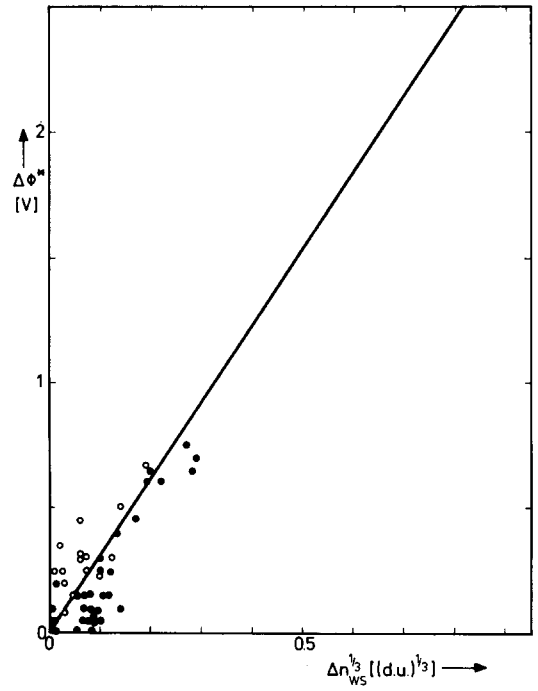

Fig. 6. Illustration of the validity of eq. (7) for the same type of liquid alloys as in fig. 5 (alloys not containing transition or noble metals) but now for those alloys for which $|\Delta H|$ has been measured to be smaller than 2.5 kJ/mole of atoms of the equiatomic composition. ○ $-2.5 < \Delta H < 0$ kJ/mole; ● $0 < \Delta H < 2.5$ kJ/mole.

signs in fig. 7 is the same as in figs. 5 and 6. The same is true for the slope of the straight line in fig. 8, where comparable information is represented for solid alloys of a transition metal and a transition, noble, alkali or alkaline-earth metal (the criteria for assigning + or − signs are somewhat different here, see figure caption).

From the data represented in figs. 5–8, we can conclude that, with a judicious choice of the parameters ϕ^* and n_{ws}, eq. (7) can be made into a powerful relation capable of predicting the sign of heats of alloy formation. Quite surprisingly, the ratio Q/P of the proportionality constants is found to be the same for widely different classes of alloy systems. Thus, relation (7) has turned out to be more universal than we had any right to expect on the basis of the way we had arrived at it.

Having separated the factor $PV_{\text{B}}^{2/3}/(n_{\text{ws}}^{-1/3})_{\text{av}}$ in eq. (7) we can also discuss the enthalpy of formation of alloys and compounds at the equiatomic composition. For this case the prefactor will involve some average of $V^{2/3}$, instead of the value appropriate to the solute B. Provided the value of this prefactor is as universal as the ratio Q/P, in a $\Delta\phi^*$, $\Delta n_{\text{ws}}^{1/3}$ diagram the loci of equal heat of formation should be represented by hyperbolae. Figs. 9a and b illustrate the graphical determination of heats of formation based on this observation. If one limits the discussion to metals with predominant s and d character in their conduction-electron states, the heats of formation can be estimated with an accuracy of about 30%. This may not seem a very impressive agreement, but it should be pointed out that the diagram gives the correct answer for a number of cases that have puzzled metallurgists for a long time. By shifting the separating lines in fig. 9a from the point corresponding to Fe

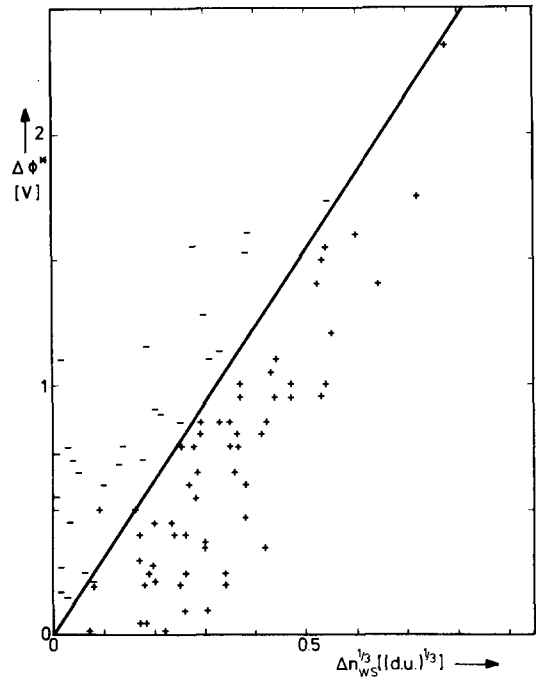

Fig. 7. Demonstration of the validity of eq. (7) for liquid alloys of transition or noble metals in combination with transition, noble, alkali or alkaline-earth metals (all these groups of metals have very little p-character in their conduction electron wave functions). The slope of the straight line that separates the + and – signs is the same as in figs. 5 and 6. The meanings of the signs are the same as in fig. 5.

along the broken line containing the points appropriate the rare-earth series, we can demonstrate that in the Fe–La system there should be no stable compounds, whereas the heavier rare-earth elements can be expected to form compounds with Fe. Such drastic differences in the chemical behaviour of various rare-earth elements are also observed in combin ation with Pu, Mn and Re, and appear to contradict the chemical similarity of rare earths. It is gratifying to observe that in the representation of fig. 9a all of the partner elements in these exceptional systems lie close to the demarcation line appropriate to La, allowing a natural explanation of the change of sign in ΔH as one moves along the rare-earth series. Other puzzling dissimilarities between seemingly similar systems include the combinations of Ni with the divalent metals Ca, Sr, and Ba. The diagram correctly reflects the experimental observation that there are stable compounds in the Ca–Ni and Sr–Ni systems, which are absent in Ba–Ni. The differences in the alloying behaviour of Ag and Au in combination with V, Cr, Nb, Ta, U, Cu and K are also reflected in the position of the two noble metals in the $\phi^*, n_{ws}^{1/3}$ map. Here we have ourselves restricted to alloys of transition metals and other metals having no p electrons. Other alloy systems (i.e. transition metals with polyvalent non-transition metals) will be discussed in section 2 below.

1.5. Earlier, related treatments of the heat of alloying

In the preceding sections we have repeatedly shown how insights gained in the study of Van der Waals substances can be used in a discussion of alloy formation. This approach is by no means new, although it may seem rather unorthodox, in view of the sharp distinction often made in textbooks between the various types of solids. In fact, Hildebrand and Scott [11] have already tried to apply the solubility parameter to mixtures of liquid metals. They found that liquid immiscibility could be quite reliably predicted for binary systems where no intermetallic compounds occur.

As a negative term was clearly needed in the formation energy in order to understand the occurrence of compounds, Mott [16] has attempted to combine the positive Hildebrand term with a negative contribution involving the Pauling electronegativities of the constituent elements. Pauling [17] had found that the heat of formation of ionic compounds was quite accurately given by

$$\Delta H = -96M(X_A - X_B)^2 \quad \text{(in kJ/mole)}, \tag{8}$$

where X_A and X_B are the electronegativities of the compounds, and M is the number of shared electron pairs. The concept of shared electrons is not applied readily to metals, but Mott worked out a rather elaborate way of determining M for binary alloys, and showed that the expression (8), together with the positive term involving the Hildebrand solubility parameter in the form $(\Delta H_{vap}/V)^{1/2}$, enabled a fairly reliable prediction of the occurrence of immiscibility in binary liquid metal systems.

The Mott–Pauling term is very similar to our first

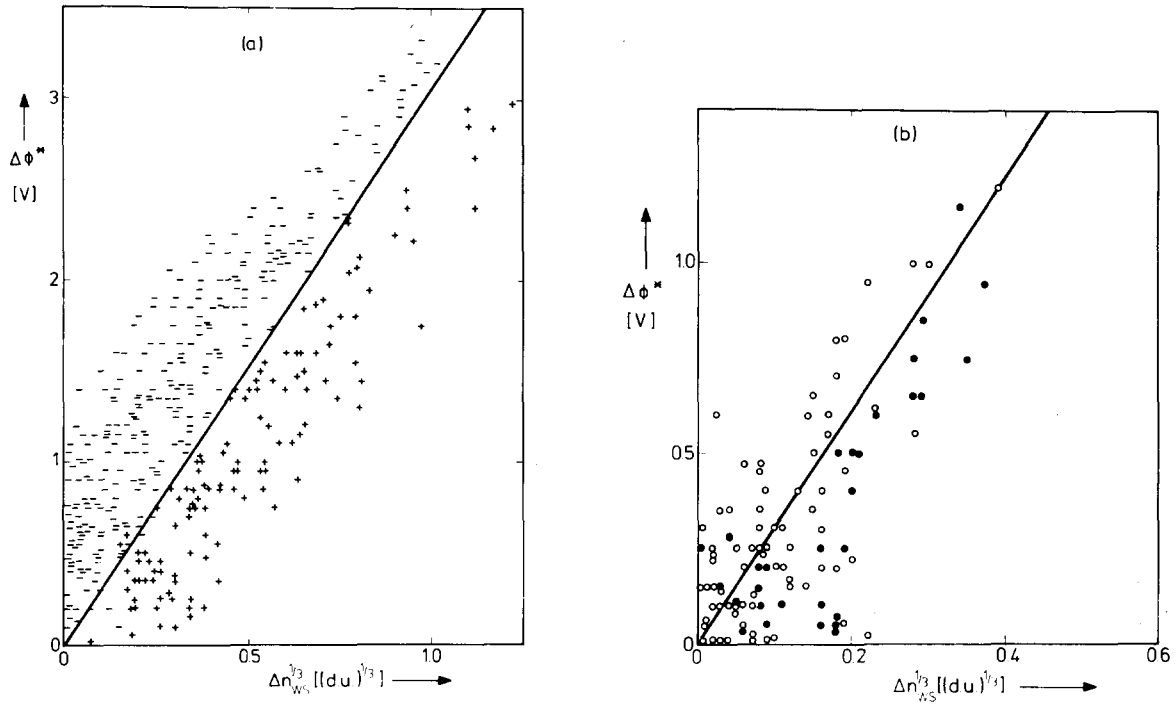

Fig. 8. Demonstration of the validity of eq. (7) for solid binary alloys consisting of a transition metal and a transition, noble, alkali or alkaline earth metal.
(a) – In the binary system one or more compounds exist, which are stable at low temperatures (indicating that ΔH is negative); + There are no compounds in the system and both solid solubilities are smaller than 10 at.% (indicating that ΔH is positive).
(b) ○ There are no compounds or ordered phases in the system, but at least one of the solubilities in the solid state is larger than 10%. It can be postulated that ΔH will not differ much from zero. This figure does indeed show that open circles mainly occur in the neighbourhood of the origin, which in the quadratic eq. (7) means that ΔH is small; ● As for the open circles, but now the solubility drops to low values at low temperatures or there is only incomplete miscibility in the solid state, although both metals have the same crystal structure. The quantity ΔH is expected to have a small but positive value.

term in eq. (7), since ϕ^* and X are approximately linearly related. This is illustrated in fig. 10, where all ϕ^* values listed in table I are plotted against the corresponding X values taken from the scale of Pauling.

Burylev and co-workers (see e.g. [18]) have used the Mott–Hildebrand approach to characterize the interaction parameters between different atoms in more complicated systems, for instance ternary alloys. Using such parameters, they have predicted with some sucess in which columns of the periodic table one finds the metals forming stable compounds with rare-earth metals, and which are the metals showing immiscibility with rare-earths. On the same basis, semiquantitative estimates of heats of mixing of various alloys were made by Sryvalin et al. [19].

A modification of the Hildebrand–Mott scheme has been recently introduced by Kumar [20]. The new feature in Kumar's scheme is the use of the heat of fusion, instead of the heat of vaporization, in the definition of the solubility parameter. Since the heat of fusion is also approximately linearly correlated with n_{WS}, it is not surprising that Kumar's solubility parameter is also useful in rationalizing immiscibility in metallic liquids. However, the accuracy of predictions based on either form of the solubility parameter is inferior to the ones based on relation (7) and illustrated in figs. 5–8.

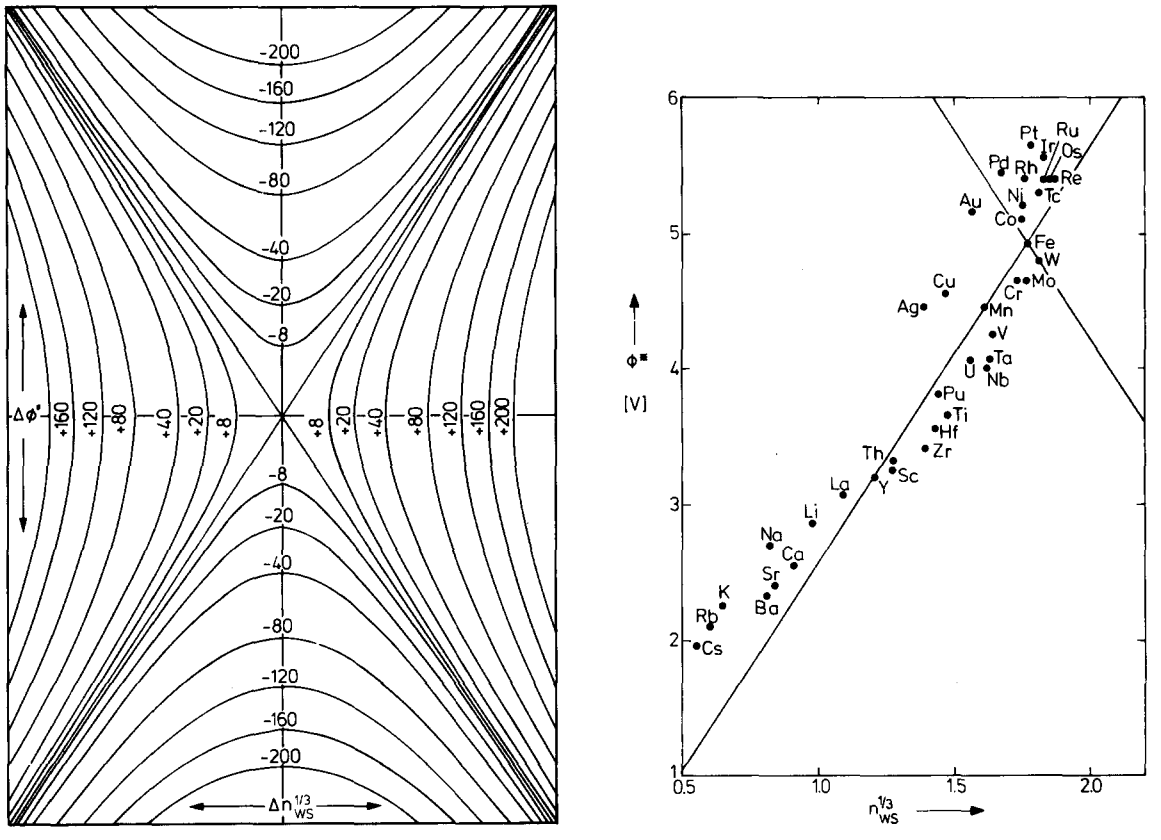

Fig. 9. (a) The values of ΔH (in kJ/mole) for an ordered solid alloy at the equiatomic composition as a function of $\Delta\phi^*$ and $\Delta n_{ws}^{1/3}$. This diagram can be used in combination with fig. 9b to estimate the heats of formation of binary alloys with the element positioned at the origin of the diagram.
(b) Graphical representation of the alloying behaviour described by eq. (7). The lines drawn separate metals that have a negative heat of alloying with Fe from metals that have a positive heat of alloying with Fe. The signs of the heats of alloying of binary alloy based on other metals than Fe can be obtained from this figure by shifting the lines in a parallel way until they pass through the desired metal. The diagram in fig. 9(a) can be used to estimate the heats of formation quantitatively by superposing a transparency of fig. 9(a) upon fig. 9(b). The slopes of the straight lines separating the + and − signs is the same as the slope of the lines in figs. 5–8

2. Numerical evaluation of ΔH

2.1. The concentration dependence

For the prediction of the sign of ΔH relation (7) is sufficient: for the sign of ΔH it makes no difference whether we consider the dilute limit (heats of solution) or concentrated alloys (heats of formation). However, as we want to evaluate heats of formation numerically, we have to specify the concentration dependence.

For arbitrary concentrations relation (7) can be rewritten as

$$\Delta H = \frac{2f(c)\,(c_A V_A^{2/3} + c_B V_B^{2/3})}{(n_{ws}^A)^{-1/3} + (n_{ws}^B)^{-1/3}} \times [-P(\Delta\phi^*)^2 + Q(\Delta n_{ws}^{1/3})^2]\,. \qquad (9)$$

In section 1.2 it has been set forth that the energy effect that accompanies alloying arises primarily from the change in boundary conditions when an atomic cell is transferred from the pure metal to the alloy. This implies that the total area of the contact surface between dissimilar atoms is the relevant quantity.

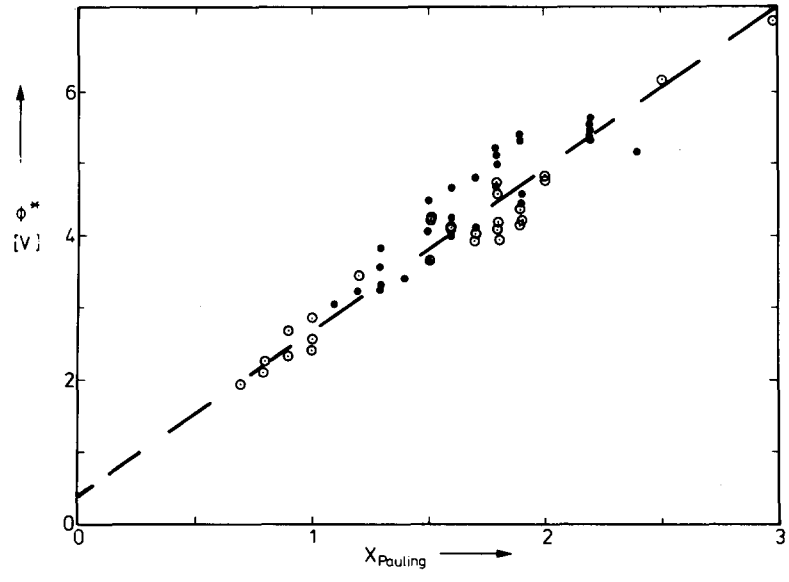

Fig. 10. Illustration of the approximate linear relationship between ϕ^* and X_{Pauling} [17].

Therefore it is useful to introduce the concept of surface concentration. For two metals A and B, in an alloy with atomic concentrations c_A and c_B and molar volumes V_A and V_B the surface concentrations c_A^s and c_B^s are defined by

$$c_A^s = c_A V_A^{2/3}/(c_A V_A^{2/3} + c_B V_B^{2/3}), \quad (10)$$

$$c_B^s = c_B V_B^{2/3}/(c_A V_A^{2/3} + c_B V_B^{2/3}).$$

For regular liquid or solid solutions the concentration function $f(c_A^s, c_B^s)$ is given by

$$f(c_A^s, c_B^s) = c_A^s c_B^s . \quad (11)$$

If the atoms of the constituent metals have equal sizes, the surface concentration, c^s, and the atomic concentration, c, are identical. For the case of atoms of different size the introduction of $f(c_A^s, c_B^s)$ leads to a ΔH function which is non-symmetric with respect to the equiatomic composition. ΔH obtains its extreme value at a concentration which is somewhat shifted from the equiatomic composition to an atomic composition which is richer in the smaller atoms.

For ordered compounds the area of contact between dissimilar atoms will be larger than the statistical value. For this case an approximation for the concentration function was obtained empirically [21] by collecting experimental data for binary systems for which experimental information about ΔH is available for a number of ordered compounds and in which size differences are small (Co–Al, Ni–Al, Cd–Mg, Cu–Zn and Pd–Al). The simplest analytical function, that is symmetrical in c_A^s and c_B^s and that describes this experimental information is

$$f(c_A^s, c_B^s)_{\text{ordered}} = c_A^s c_B^s \, [1 + 8(c_A^s c_B^s)^2], \quad (12)$$

It must be stressed that this expression has no further physical significance than that it approximates the concentration dependence of the heat of formation of ordered compounds.

The two concentration functions given in eqs. (11) and (12) are compared in fig. 11. For convenience we assumed the two types of metal atoms to have equal sizes. In the dilute cases, i.e. for compositions AB_n or A_nB with $n \gg 1$, the two concentration functions coincide. This is in accordance with a contact interaction picture in which only the degree to which a given atom is surrounded by dissimilar neighbours matters. In the dilute limit, both in disordered and ordered phases the minority-component atoms are entirely surrounded by dissimilar atoms, and hence the two curves coincide. The common slope at $c = 0$ gives

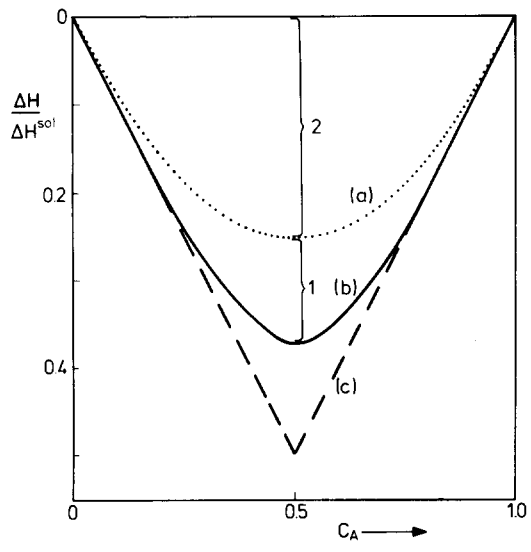

Fig. 11. The average concentration dependence of the heat of formation of a series of intermediate phases in a binary system. The figure applies to metals of equal volumes. If volumes are different it can still be used if c_A is replaced by the surface concentration c_A^s. Curve (a) is the concentration dependence for regular solutions (eq. (11)). Triangle (c) represents the other extreme (each atom completely surrounded by dissimilar neighbours). Curve (b) is a curve for ordered compounds which has been obtained empirically [21] and is represented by eq. (12).

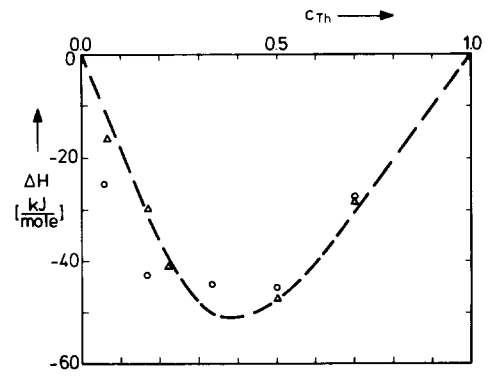

Fig. 12. The concentration dependence of the heat of formation of ordered compounds in the systems Th–Co (triangles) and Th–Ni (circles) [22]. The dashed curve is the average of the calculated heats of formation of the Th–Co and Th–Ni systems.

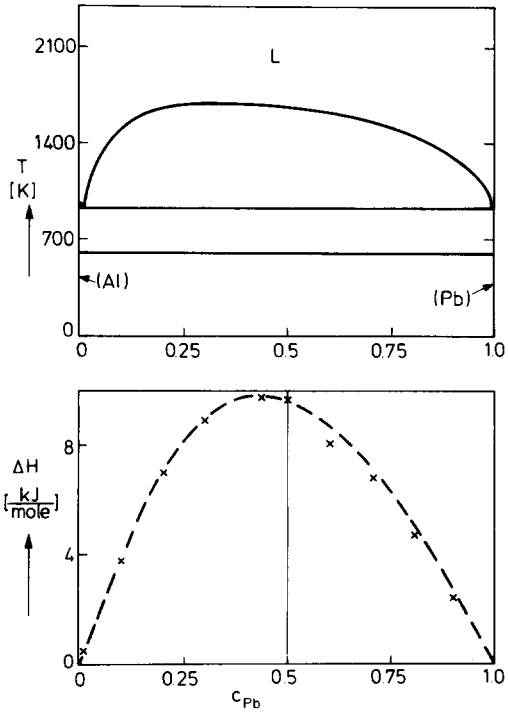

Fig. 13. The phase diagram for the system Al–Pb and the heat of mixing at 1200 K. The dashed curve represents the calculated values. The experimental data have been taken from ref. 23.

the value for the heat of solution. The relative difference of the two concentration functions at $c = 0.5$ is in agreement with experimental information on the heat of ordering of alloys of equiatomic composition that have an ordering temperature in the solid range: as an average, the heat of ordering corresponds to about one third of the heat of formation of the ordered alloy.

In fig. 12 is shown how the introduction of the surface concentration opens the possibility to describe the asymetric enthalpy of formation curves. As examples we chose the binary systems Th–Co and Th–Ni, which consist of atoms of widely different size (see table I).

It should be pointed out that a non-symmetrical concentration dependence of ΔH can also occur for liquids and that it can as well occur if ΔH is positive. This is illustrated in fig. 13 where we have plotted the heat of mixing of liquid Al–Pb alloys.

2.2. Volume effects

In the calculations of ΔH we have used values for $V_m^{2/3}$ which were derived from volume data for the pure solid elements at room temperature. For the elements Si, Ge, Sb and Bi a correction has been applied to account for the fact that as pure elements they crystallize in open structures, having molar volumes somewhat larger than they will have in metallic alloys. Obviously, this has to do with their semiconducting, semi-metallic character that generally is associated with a volume expansion upon solidification.

In the calculation of the heat of mixing of liquid alloys Boom et al. [15] have used the values for $V_m^{2/3}$, ϕ^* and $n_{ws}^{1/3}$, as derived for the solid metals. That this approximation is correct can be seen as follows. The numerator in eq. (9) is proportional to $V_m^{2/3}$, the denominator is proportional to $n_{ws}^{-1/3}$. If a metal expands, i.e. if V_m increases, the n_{ws} decreases and $n_{ws}^{-1/3}$ increases, so that the overall effect is zero in first approximation. The effect is small as long as

$$\frac{V_m}{n_{ws}} \frac{dn_{ws}}{dV_m} \simeq 2, \tag{13}$$

which is particularly the case for transition metals [24].

At this point we note that eq. (9) may lead to large volume contractions in the special case that we are concerned with alloys with a large, negative heat of formation in which the majority metal is an easily compressible one. Examples of such alloys are $AuLi_3$, $SbCs_3$ and $PbCa_3$. Here the first metal A (Au, Sb, Pb) is completely surrounded by B (Li, Cs or Ca). In these cases the numerator of eq. (9) is proportional to $V_A^{2/3}$ and independent of $V_B^{2/3}$ (to see this, we assume regular-solution behaviour, substitute eqs. (11) and (10) into (9), and make use of the fact that A is the minority metal, that is, $c_A \ll c_B$). The bulk modulus and n_{ws} being strongly correlated [10], the easily compressible partner B will have to lower n_{ws}, and the denominator of eq. (9) will be dominated by $(n_{ws}^B)^{-1/3}$. Thus, if ΔH is negative, a contraction of metal B lowers the total energy. From eq. (7) or (9) the volume contraction of metal B can be estimated to be

$$\Delta V_B / V_B = (2/3)\, \Delta H_{int} / c_B V_B B_B, \tag{14}$$

where ΔH_{int} is the integral heat of formation per mole alloy atoms, and B_B the bulk modulus of metal B. In accordance with this expression, the largest effects are observed in alloys where a low-valence metal is the majority component [25]. For such metals the product BV_m is found to be very small (see table I).

Other, quite generally occurring volume effects (indirectly related to a negative ΔH) are connected with the $(\Delta\phi^*)^2$ term. When a dipole layer is generated at the contact surface between two metals, charge is transferred from the metal where electrons have a high chemical potential to the metal with the lower potential. If the two metals also have different electron densities then the charge transfer is accompanied by a volume effect

$$\Delta V_m \propto \Delta z / [(n_{ws}^A)^{-1} - (n_{ws}^B)^{-1}] \propto \Delta\phi^* / \Delta(n_{ws}^{-1}). \tag{15}$$

Quite generally the metal with the higher ϕ^* value also has the higher value for n_{ws}, so that a volume concentration will be the result. The proportionality constant in eq. (15) will depend on the composition and on the degree to which in a compound of a given composition the one kind of atom is surrounded by the other kind, which is determined by the crystal structure. If other volume effects are absent one would expect the proportionality constant in eq. (15) to increase regularly in the sequence AB, AB_2, AB_3. To illustrate the validity of eq. (15) we show in fig. 14 the experimentally observed volume contractions for compounds of two transition metals with the results of eq. (15). Also, the slope of the straight line drawn increases regularly in the sequence AB, AB_2, AB_3. We must note that the fair agreement in fig. 14 is partly due to the fact that we have considered only one structure and not one composition, so that structure dependent volume effects have been excluded.

The observed volume contractions are the net effect of two effects of opposite sign: in the charge transfer picture one type of atoms contracts while the other expands. Hence individual changes in atomic volume can become quite large which may affect the value of the concentration function $f(c^s)$. In earlier papers [13–15] we have presented an approximate, simple to handle, relationship to find the values for the individual values of $V_m^{2/3}$ including the charge transfer:

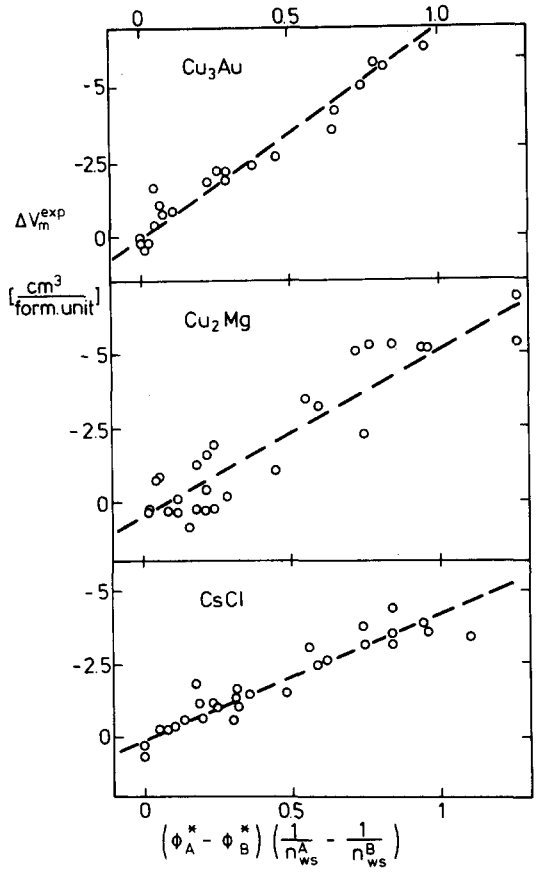

Fig. 14. Volume contraction in intermetallic compounds of two transition metals with the Cu_3Au, Cu_2Mg and CsCl structures. The observed volume contractions (derived from the data in ref. 27) correlate well with those expected to result from charge transfer effects.

$$V_A^{2/3}(\text{in alloy}) = V_A^{2/3}(\text{pure A}) \times \{1 + a f_B^A (\phi_A^* - \phi_B^*)\}, \quad (16)$$

where f_B^A is a measure of the degree to which A atoms are surrounded by B atoms and "a" is a constant, derived from experimental volume contractions in compounds ($a = 0.14$ for the alkali metals, $a = 0.10$ for the divalent metals, $a = 0.07$ for trivalent metals and Cu, Ag, Au and $a = 0.04$ for all other metals). For statistical liquid or solid solutions of equal size atoms $f_B^A = c_B$. In the past we have used this result for unequal atomic sizes and ordered alloys, too, which is a crude approximation. Although in practice the difference is not large we prefer in this paper the more correct expressions

$$f_B^A = c_B^S \quad \text{for solutions}$$
and
$$f_B^A = c_B^S \{1 + 8 (c_A^S c_B^S)\} \quad \text{for ordered alloys.} \quad (16a)$$

Only for alloys with large values of $\phi_A^* - \phi_B^*$ is the correction of significance.

2.3. Predictions for ΔH

2.3.1. Alloys of two transition metals

In the numerical evaluation of ΔH we need values for the proportionality constants P and Q in eq. (9). From figs. 5–8 it follows that both for liquid alloys and solid compounds of two transition metals the value for Q/P (which can be obtained from the slope of the straight lines in the figures) equals $9.4\ V^2/(\text{d.u.})^{2/3}$.

A value for P can be found by comparison of the available experimental data (which are numerous since for instance the 30 transition and noble metals of table Ia present (30 X 29)/2 binary alloy systems) with relationship (9). We do not repeat the comparison here but refer to the original papers [14, 15]. Expressing in relation (9) ϕ^* in volts, n_{ws} in the density units of table I, V_m in cm^3 and enthalpies in kJ/mole, we have for alloys of two transition metals (both solid and liquid) $P = 14.1$.

A representative selection of heats of solution of transition–transition metal and transition-noble metal systems calculated with this P value have been collected in table II. The heat of formation of an ordered compound of equiatomic composition can be directly obtained by multiplication of the average of the two heat of solution values by 0.375 (see fig. 11).

Large positive heat of solution values exceeding 100 kJ/mole, which are connected with a limited solid solubility, occur for instance for Ag in Cr, Fe or W and for the rare-earth metals and Y in W. A value of 100 kJ/mole for the heat of solution at for instance 100 K leads via $c = \exp(-\Delta H^{sol}/kT)$ to a solubility of 10^{-5}, which gives an impression of the strength of the repulsive interactions that can occur in some transition metal combinations.

A way to get some feeling for the magnitude of

Table II
Heats of solution for (liquid) binary alloys of two transition metals (kJ/mole solute)

	Solvent														
	Ti	V	Cr	Mn	Fe	Co	Ni	Cu	Y	Ru	Pd	Ag	W	Pt	Au
Ti	–	−9	−38	−46	−82	−140	−170	−78	+40	−191	−283	−55	−25	−313	−210
V	−8	–	−8	−3	−29	−58	−75	+16	+54	−94	−131	+48	−3	−167	−69
Cr	−32	−8	–	+8	−6	−18	−27	+52	+35	−42	−52	+85	+3	−86	−1
Mn	−39	−3	+9	–	+1	−21	−33	+14	−5	−40	−82	+37	+23	−101	−40
Fe	−70	−28	−6	+1	–	−2	−6	+60	−4	−17	−16	+94	−0	−47	+28
Co	−115	−53	−17	−20	−2	–	−1	+35	−67	−3	−5	+63	−5	−25	+25
Ni	−140	−69	−26	−32	−6	−1	–	+26	−97	+2	−0	+52	−11	−17	+25
Cu	−67	+15	+52	+14	+58	+35	+25	–	−91	+40	−33	+4	+86	−24	−20
Y	+58	+85	+58	−8	−6	−112	−161	−148	–	−157	−377	−154	+110	−365	−316
Ru	−187	−104	−50	−46	−20	−3	+2	+49	−113	–	+24	+88	−39	−4	+57
Pd	−293	−152	−65	−101	−19	−7	−0	−43	−287	+25	–	−25	−26	+8	+0
Ag	−60	+57	+108	+46	+116	+80	+66	+5	−121	+92	−25	–	+161	−1	−18
W	−26	−3	+4	+28	−0	−6	−14	+107	+81	−40	−26	+156	–	−79	+44
Pt	−337	−200	−111	−129	−59	−33	−22	−32	−291	−4	+8	−1	−83	–	+17
Au	−247	−89	−1	−54	+38	+34	+34	−29	−274	+65	+0	−20	+49	+18	–

negative ΔH-values is to calculate the temperature rise which would occur in an adiabatic reaction. The ΔH^{sol}-values for Pd, Pt, or similar metals with metals like Sc and Ti are as large as −300 kJ/mole which means that the heat of formation for an equiatomic compound amounts to −115 kJ/mole. Such a heat effect produces in an adiabatic reaction a temperature rise of $115 \times 10^3/3R = 4600$ K.

There is a wealth of experimental information on the very stable compounds of two transition metals. Brewer and Wengert [28] explain the high stability of transition metal alloys in terms of the Engel–Brewer theory in which stability is related to the number of electron pairs contributing to the bonding between dissimilar atoms. High stability is expected if a metal with some completely vacant 4d- or 5d-orbitals is combined with a metal with an almost completely filled 4d- or 5d-shell. The starting point from the Engel–Brewer model is quite different from that of the macroscopic atom model and it seems to be impracticable to establish a relationship between both models.

2.3.2. Alloys of two non-transition metals

In section 1.4 we have shown that there is no difference in the sign analysis of the heat of formation of liquid alloys of two non-transition metals (figs. 5 and 6) and of liquid alloys of two transition metals (fig. 7) i.e. the value of Q/P is identical for these two types of alloys.

On the other hand, collecting the available experimental data on heats of solution and heats of mixing, Boom et al. [15] have found that for non-transition metal alloys P has a 30% smaller value than for transition metal alloys. Since the ratio Q/P is identical for the two types of alloys, the Q values are also expected to differ by 30%.

This difference between the Q values for transition and non-transition metals is also reflected in fig. 15, taken from ref. 6, which demonstrates that there exists an approximate linear relationship between γ_s^0/n_{ws} and $(n_{ws}/\bar{n})^{3/5}$, where $\bar{n}$ represents the average electron density in the atomic cell. As shown in fig. 15 for non-transition metal alloys, the proportionality constant between γ_s^0/n_{ws} and $(n_{ws}/\bar{n})^{3/5}$, which is a measure for Q (ref. 6), is indeed 30% smaller than for transition metal alloys.

A representative selection of heats of solution for combinations of two non-transition metals has been collected in table III. The variation in ΔH values is large; the values tend to be more positive than those in table II for transition metals.

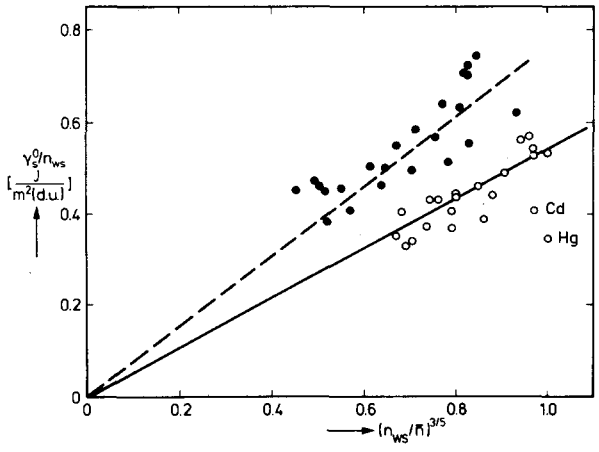

Fig. 15. The approximate linear relationships between γ_s^0/n_{ws} and $(n_{ws}/\bar{n})^{3/5}$ for transition metals (filled circles) and non-transition metals (open circles). Here $\bar{n}$ equals the average electron density.

In our previous papers solid alloys of two non-transition metals were not considered for the following reasons. In the contact interaction model structure dependent energy contributions are not taken into consideration. Only an empirically obtained structure independent concentration function (section 2.1.) accounts for the effect that in ordered compounds the area of contact between dissimilar atoms will be larger than the statistical value. Effects of the optimal filling of Brillouin zones in k-space, giving rise to some energy lowering for the phases that eventually are the stable ones in a given binary system are neglected. Apparently this is permitted for transition metals, as is proved by the completely equivalent model description for solid and liquid alloys. In other words the structure-dependent contribution to the cohesive energy of a solid transition metal alloy is not much different from the average of structure-dependent contributions to the cohesive energies of the constituent pure metals. Since the heats of fusion of the transition metals are not very large, this is not very surprising. If we consider the entropy of fusion rather than the enthalpy of fusion it is not far from a constant value of 9.5 J K^{-1} $mole^{-1}$, for all transition metals (see fig. 16).

For non-transition elements one must distinguish between semiconductors and semimetals on the one hand and ordinary metals on the other. For the majority of the non-transition metals the heat of fusion is small, with $\Delta S_f \simeq 10$ J K^{-1} $mole^{-1}$. The elements Si, Ge, Sb and Bi are exceptions from this general rule.

The deviating structure-dependent energy of semiconductors has two consequences. In the first place the heat of formation of alloys or compounds containing Si, Ge (and Sb) will be less exothermic (less

Table III
Heats of solution for (liquid) binary alloys of two non-transition metals (kJ/mole solute)

	Solvent													
	Li	Na	Cs	Be	Mg	Zn	Al	In	Si	Ge	Sn	Pb	Sb	Bi
Li	–	+12	+43	+104	−1	−26	−13	−41	−46	−75	−56	−67	−85	−71
Na	+17	–	+8	+265	+45	+28	+58	−21	+24	−39	−31	−64	−72	−69
Cs	+103	+13	–	+536	+145	+93	+153	−19	+82	−40	−35	−116	−115	−125
Be	+77	+135	+166	–	+53	+33	+19	+71	−7	+17	+53	+80	+45	+77
Mg	−1	+38	+73	+92	–	−15	−8	−14	−39	−58	−31	−28	−57	−33
Zn	−28	+21	+42	+49	−13	–	+2	+10	−3	−11	+3	+16	−3	+14
Al	−15	+45	+71	+30	−7	+2	–	+23	−9	−8	+14	+33	+8	+31
In	−59	−20	−11	+148	−17	+14	+31	–	+32	−4	−1	−3	−14	−5
Si	−51	+18	+37	−11	−34	−4	−9	+23	–	+9	+21	+48	+28	+47
Ge	−88	−32	−19	+28	−54	−12	−8	−3	+10	–	−0	+16	+6	+16
Sn	−83	−32	−21	+117	−38	+5	+19	−1	+30	−0	–	+6	−5	+5
Pb	−106	−70	−74	+187	−37	+25	+49	−3	+75	+23	+6	–	+2	−0
Sb	−138	−80	−75	+105	−74	−5	+11	−15	+43	+8	−5	+2	–	+3
Bi	−120	−80	−84	+189	−45	+23	+48	−6	+78	+24	+6	−0	+3	–

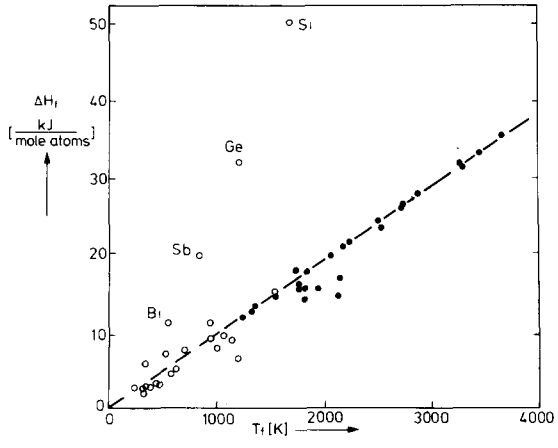

Fig. 16. The approximate linear relationship between the heat of fusion, ΔH_f, and the temperature of fusion, T_f, for metals (data from ref. 23). The straight line drawn corresponds to an entropy of fusion of 9.5 J K^{-1} $mole^{-1}$. The black dots represent transition metals, the open circles non-transition metals. The semi-conducting and semi-metallic elements deviate seriously from the general trend.

negative), since in general the energy gain due to the optimal filling of the Brillouin zones will be larger in the pure elements than in the alloys. On the basis of estimates of the structure-dependent energies the heat of formation of alloys containing Si, Ge, must be increased by an amount of 34 and 25 kJ/mole, respectively. For Sb and Bi the correction has not been applied. It is small and partly included in the value of R, see section 2.3.3. Secondly, if a semiconducting compound is formed from two ordinary metals there can be an additional negative contribution to the heat of formation. This effect is for instance manifest in Mg_2Sn.

The presence of structure dependent energy contributions in alloys of two non-transition metals is illustrated in figs. 17 and 18. In both figures the dashed line is the same as the one found in figs. 5–8 for the liquid and solid systems considered there. In fig. 18 solid non-transition metal alloys are analysed that contain at least one alkali metal; in fig. 17 one finds the remaining solid binary combinations of two non-transition metals.

One will notice in fig. 17 that there are a lot of plus signs in the region where only negative signs are expected and also some minus signs in the positive region. These "exceptions" are listed in table IV. The result is quite reassuring. In all cases where the heat of formation does not have the expected negative sign, either Si or Ge is involved, which explains the deviating behaviour. For at least three of the five systems which are negative in the positive region semiconducting behaviour with a large gap is likely: Be_3Sb_2 in the Be–Sb system, AlSb in the Al–Sb system and $SiAs_2$ in the Si–As system.

In fig. 18 we have drawn a second straight line, which properly separates plus and minus signs. The systems in between the two lines are considered in detail in table IV. Again, there is reason to qualify

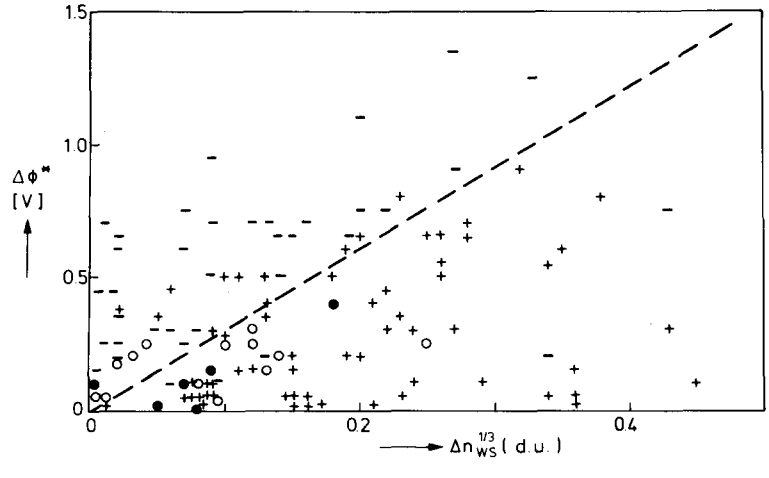

Fig. 17. The sign of the heat of formation of binary solid alloys of two non-transition metals excluding alkali metals. For the meani of the symbols we refer to the caption to fig. 8. The slope of the dashed line is the same as in figs. 5–8.

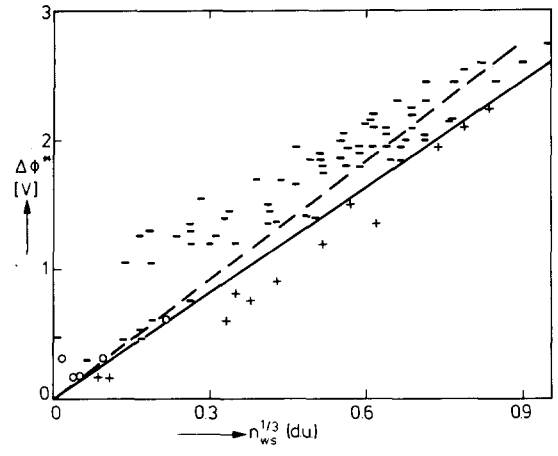

Fig. 18. The sign of the heat of formation of binary solid alloys of two non-transition metals of which at least one is an alkali metal. For the meaning of the symbols we refer to the caption to fig. 8. The solid line separates the plus and minus signs; the dashed line is that of figs. 5–8 and 17.

them as exceptional. There is a group of systems in which there is only one compounds with a very large coordination number. Here K–Zn is a representative: the only compound is KZn_{13} while for the liquid the heat of mixing appears to be large and positive (fig. 19). A fairly small, structure dependent, energy term must be responsible for the existence of the single compound at low potassium contribution. Similar systems are other alkali metals with Zn and also with Cd.

In the systems Na–K and Na–Cs, too, there is only one compound and one may also ascribe the existence of Na_2K and Na_2Cs to a (small) structure dependent energy term, reflecting the increase in coordination number in a Laves phase. For liquid Na–K and Na–Cs the enthalpy of mixing has the positive sign; in the solid ΔH is lowered by about 1 kJ/mole, which is sufficient to make it negative.

For the remaining systems of table IV (alkali metals with Ga or Si) we suggest Brillouin zone effects to play a role. An indication for this is found in the phase diagrams [29, 30]. While (fig. 19) the compound KGa_4 and K_5Ga_8 are fairly stable, there is immiscibility for liquid K–Ga alloys. Also, the experimental value of the entropy of fusion of Na_5Ga_8 has been reported as 19 J/K, which is nearer to the value for Sb than to that for an ordinary metal.

As a matter of fact, the compounds of table IV are not the only ones in which structural energies add to the stability. For the compounds of table IV there is

Table IV
The exceptions in figs. 17 and 18. Solid binary combinations of two non-transition metals, that do not exhibit the sign of ΔH as predicted by eq. (9). The phase diagram information is from refs. 29–31

– in the + region fig. 17	+ in the – region fig. 17	– in the + region fig. 18	Compounds observed
Be–Sb	Be–Si	K–Zn	KZn_{13} only
Al–Sb	Be–Ge	K–Cd	KCd_{13} only
Be–Mg	Zn–Ge	Rb–Zn	$RbZn_{13}$ only
Si–As	Cd–Ge	Rb–Cd	$RbCd_{13}$ only
	Al–Si	Cs–Cd	$CsCd_{13}$ only
	Al–Ge	Na–Zn	$NaZn_{13}$ only
	Ga–Si	Na–K	Na_2K only
	Ga–Ge	Na–Cs	Na_2Cs only
	In–Si	Na–Ga	$NaGa_4$; Na_5Ga_8
	In–Ge	K–Ga	KGa_4 ; K_5Ga_8
		Rb–Ga	$RbGa_4$; Rb_5Ga_8
		Cs–Ga	$CsGa_4$; Cs_5Ga_8
		Na–Si	$NaSi$; $NaSi_2$
		K–Si	KSi ; KSi_2
		Rb–Si	$RbSi$; $RbSi_6$
		Cs–Si	$CsSi$; $CsSi_8$

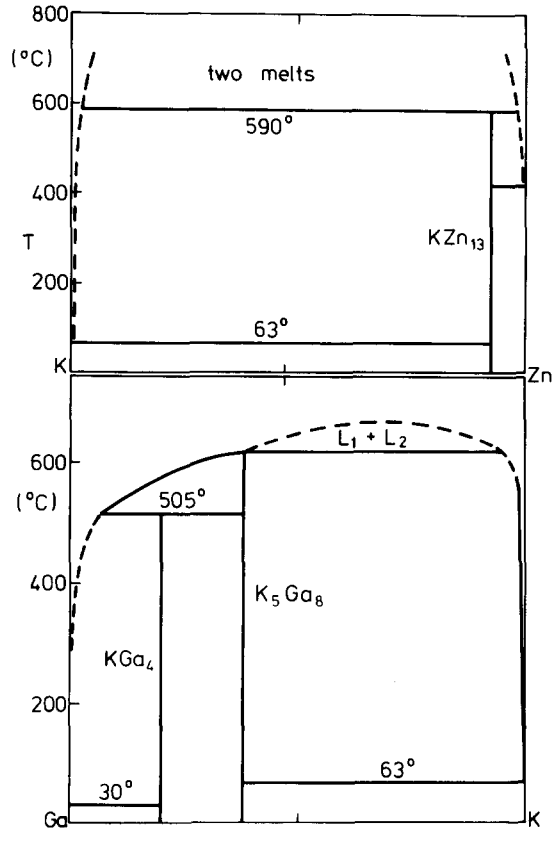

Fig. 19. Phase diagrams of two of the systems listed in table IV that form exceptions to the simple two-term description of the heat of formation. From the phase diagrams it is understandable why these systems are exceptional (see text).

a change in the sign of ΔH; if the numerical value is only lowered the system is not noted to be an exceptional one. Some indication how large Brillouin zone effects can be, and to which extent they can be predicted, is given in fig. 20. Here we have plotted for three types of semiconductors all having 8 electrons per formula unit (i.e. GaSb-type, Mg_2Sn-type and Na_3Sb-type) the observed energy gap, ΔE_g, in the electronic density of states curve versus the apparent additional part of the heat of formation. The gap is the one observed at room temperature; the structure dependent part of the heat of formation is obtained by comparing the value calculated from relation (9) with the experimentally observed one. The experimental uncertainty is large in both ΔE_g and $\Delta H_{exp} -$

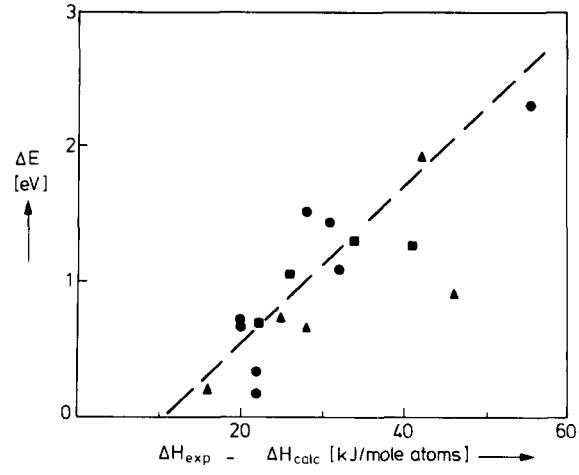

Fig. 20. The correlation between the structure dependent part of the heat of formation of intermetallic compounds of two non-transition metals and the semiconducting energy gap. Experimental data on ΔH are from ref. 23, data on ΔE_g from refs. 32–34. The negative intercept of the extrapolated line with the ΔE_g axis is presumably due to the fact that optically one detects the smallest possible gap, whereas for the binding energy the average gap is relevant.

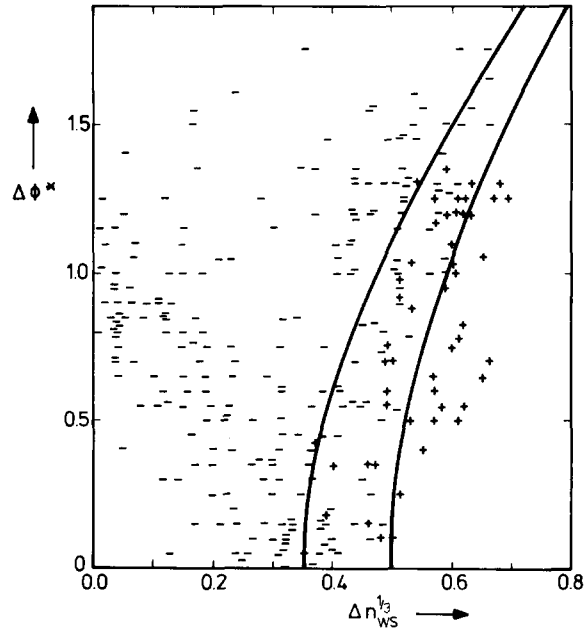

Fig. 21. Analysis of the sign of ΔH for solid alloys of a transition metal and one of the metals Al, Ga, In, Tl, Sn, Pb, As, Sb and Bi.

ΔH_{calc}. However, one tends to conclude from fig. 20 that (1) structure dependent energy terms to a good approximation can be treated as additive to the "metallic" terms, (2) large structure dependent energy terms are accompanied by semiconducting electronic properties.

2.3.3. Alloys of transition metals with non-transition metals

From the analysis of the sign of the heat of formation of solid alloys of transition metals with non-transition metals, similar to that of figs. 5–8, it was found that relations (7) or (9) with only two energy terms were not sufficient. If a transition metal is alloyed with a non-transition metal having p-electrons, there is a large negative contribution to the heat of formation that does not depend much on which transition metal is alloyed with which p-metal partner. The idea becomes clear from fig. 21. The figure gives the sign of the heat of formation for alloys of an arbitrary transition metal combined with one of the polyvalent non-transition metals. It is possible to separate regions of positive and negative signs by a demarcation region. However, this demarcation region has a hyperbolic shape, very different from the straight line we had before. The sign of ΔH apparently can be approximately described by an expression of the form

$$\Delta H \sim -P(\Delta\phi^*)^2 + Q(\Delta n_{ws}^{1/3})^2 - R. \qquad (17)$$

The hyperbolae drawn give a value for both Q/P and R/P. That for Q/P is the same as found before for alloys for which $R = 0$.

A more detailed analysis, as shown in fig. 22 demonstrates a systematic (weak) dependence of the value of R on the valence of the polyvalent non-transition metal. The larger the number of p-electrons, the larger R. A survey of the appropriate values of R for various combinations of metals is given in fig. 23.

Boom et al. [15] have shown that also for liquid metals the R term is present, albeit reduced by a factor of 0.73 (average value). The fact that R is present in the liquid as well as in the solid proves that it is a term different from the Brillouin zone filling type effects discussed above. It can be treated as a third contact interaction energy contribution. If a metal atom with d-type wave functions has a metal atom offering p-type wave functions as its nearest neighbour, the result is an energy lowering. If ascribed to a type of d–p electron hybridisation effect, the gradual change of the R-values with number of p-electrons is to be expected. Also the fact (fig. 23) that R is small but significant for Cu, Ag and Au at the right hand side of a transition metal series and for alkaline-earths and rare-earths metals on the left hand side is the behaviour one expects. Even the difference between Cu and Au at the one hand and Ag on the other (which came out as a result of the analysis of a large number of experimental numerical data) is quite easy to accept in view of the much lower energy of the d states in Ag.

In the predictions of ΔH values for the present group of alloys we use the full expression

$$\Delta H = \frac{2P f(c^s)\,(c_A V_A^{2/3} + c_B V_B^{2/3})}{(n_{ws}^A)^{-1/3} + (n_{ws}^B)^{-1/3}} \times \left[-(\Delta\phi^*)^2 + \frac{Q}{P}(\Delta n_{ws}^{1/3})^2 - \frac{R}{P}\right]. \qquad (18)$$

A representative selection of values of the heat of solution of transition metals in liquid non-transition metals is given in table Va. Since for solid and liquid alloys the R-values differ there is no direct connection between heats of solution and the heat of formation of ordered compounds. We therefore add table Vb, giving ΔH for AB compounds. Note that due to the difference in the R value there now can be a change in the sign of ΔH upon going from the liquid to the solid state. A well-known example here is the system Fe–Sn, in which there is liquid immiscibility over a wide range of concentrations but there are several stable intermetallic compounds.

Alloys of transition metals with Si, Ge, C, N and B can be treated like the other alloys of transition metals with polyvalent non-transition metals. The only difference is that for C, Si and Ge there is an additional positive contribution to account for the enthalpy difference between these elements in the diamond structure and a more conventional metallic structure. For Si and Ge this positive contribution is 34 and 25 kJ per mole Si and Ge, respectively. For carbides the corresponding transformation energy equals 100 kJ per mole.

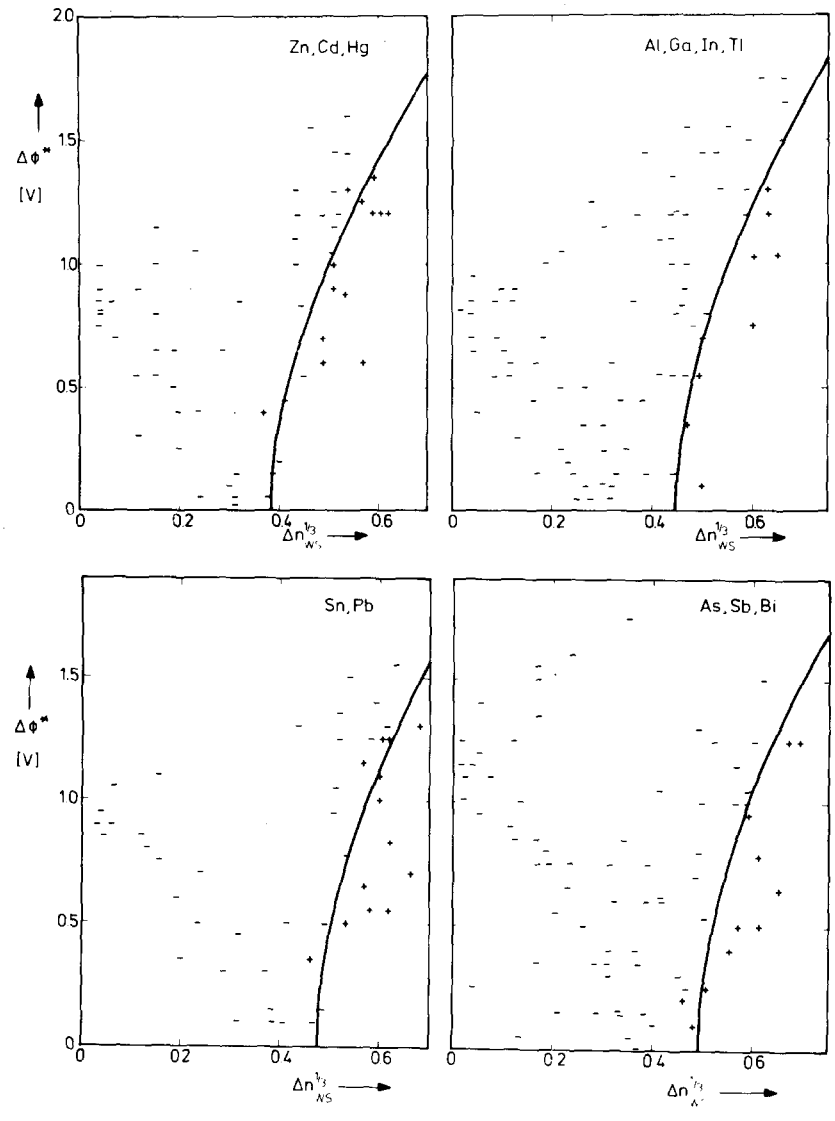

Fig. 22. Determination of the value of the constant R in relation (17) for alloys in which a transition metal is combined with a non-transition metal with p-electrons. Systems for which ΔH is negative are separated from those for which ΔH is positive by a hyperbola. For all four groups the same value of Q/P applies, that of figs. 5–8. It can be seen that R increases with the number of valence electrons of the p-metal.

Also nitrides of transition metals can be treated as metallic alloys. There is an additional positive term that represents the enthalpy difference between molecular N_2 (at room temperature) and the imaginary metallic form of nitrogen. This term was found to be 240 kJ/g-at N [14], [35]. It is interesting to note that such a value implies that metallic nitrogen will be quite stable relative to free nitrogen atoms.

An extensive comparison of predictions and experimental data on ΔH of transition metal silicides, germanides, carbides, nitrides and borides has been made elsewhere [14, 35]. The agreement observed is quite encouraging.

TRANSITION METALS

Ca 0.4	Sc 0.7	Ti 1.0	V 1.0	Cr 1.0	Mn 1.0	Fe 1.0	Co 1.0	Ni 1.0	Cu 0.3
Sr 0.4	Y 0.7	Zr 1.0	Nb 1.0	Mo 1.0	Tc 1.0	Ru 1.0	Rh 1.0	Pd 1.0	Ag 0.15
Ba 0.4	La 0.7	Hf 1.0	Ta 1.0	W 1.0	Re 1.0	Os 1.0	Ir 1.0	Pt 1.0	Au 0.3

Th 0.7	U 1.0	Pu 1.0

NON-TRANSITION METALS

Li 0	Be 0.4	B 1.9	C 2.1	N 2.3
Na 0	Mg 0.4	Al 1.9	Si 2.1	
K 0	Zn 1.4	Ga 1.9	Ge 2.1	As 2.3
Rb 0	Cd 1.4	In 1.9	Sn 2.1	Sb 2.3
Cs 0	Hg 1.4	Tl 1.9	Pb 2.1	Bi 2.3

PHASE

SOLID 1.0
LIQUID 0.73

Fig. 23. The value of the parameter R in relations (17) and (18) (or in fact R/P in units V^2) for alloys of transition metals with polyvalent non-transition metals is obtained by multiplying 3 numbers: One out of the block of transition metals, one out of the block of non-transition metals and one for solid or liquid phase. As an example for solid compounds of Cr and Sn the value of $R/P = 2.1\ V^2$; for liquid alloys of Al and Ag R/P equals (0.73) (1.9) (0.15) = 0.21 V^2. For all alloy systems Q/P equals 9.4 V^2/(d.u.)$^{2/3}$. The values for P, used in calculating numerical values for ΔH are P = 14.1, 10.6 and 12.3 (ϕ^* in volt, n_{ws} in density units, V_m in cm^3, enthalpies in kJ/mole) for alloys of two transition metals, two non-transition metals and a transition metal with a non-transition metal, respectively. As far as the value of P is concerned, alkaline-earth metals are non-transition metals.

Table Va
The heat of solution of liquid transition metals in a number of liquid non-transition metals (kJ/mole solute)

	Solute											
	Y	Ti	V	Cr	Fe	Co	Ni	Mo	Pd	Cu	Ag	Au
Li	+37	+116	+140	+126	+96	+30	+3	+193	−165	−38	−74	−168
Na	+108	+199	+230	+218	+196	+125	+100	+307	−50	+30	−1	−53
Mg	−27	+40	+82	+81	+61	+10	−12	+133	−153	−29	−47	−131
Zn	−151	−82	−6	+18	+14	−19	−34	+49	−140	−20	−19	−75
Al	−181	−135	−61	−36	−41	−68	−81	−20	−187	−32	−22	−95
Ga	−179	−109	−29	−2	−6	−38	−53	+25	−164	−25	−22	−80
In	−147	−46	+40	+66	+63	+21	+5	+113	−112	+0	−4	−41
Tl	−138	−22	+71	+99	+99	+56	+41	+155	−72	+19	+14	−6
Sn	−203	−100	−3	+32	+34	+1	−12	+69	−118	−8	−8	−38
Pb	−184	−58	+48	+86	+92	+53	+40	+138	−62	+18	+15	+8
Sb	−264	−143	−25	+23	+33	+6	−4	+57	−95	−7	−8	−14
Bi	−205	−77	+33	+73	+80	+43	+31	+122	−26	+15	+12	+6

Table Vb
The heat of formation of equiatomic compounds of a transition metal and a non-transition metal (kJ/mole atoms)

	Y	Ti	V	Cr	Fe	Co	Ni	Mo	Pd	Cu	Ag	Au
Li	+11	+44	+55	+50	+38	+12	+1	+71	−58	−15	−26	−53
Na	+41	+88	+104	+100	+89	+57	+46	+135	−21	+14	−0	−22
Mg	−12	+13	+31	+32	+23	+1	−8	+50	−63	−13	−19	−49
Zn	−54	−42	−13	−3	−5	−18	−23	+6	−59	−11	−8	−28
Al	−68	−67	−40	−30	−32	−42	−48	−24	−84	−17	−10	−37
Ga	−73	−60	−28	−16	−18	−31	−37	−7	−79	−15	−11	−34
In	−67	−36	+2	+14	+13	−5	−12	+31	−63	−4	−4	−21
Tl	−65	−26	+16	+30	+30	+11	+4	+50	−47	+4	+3	−8
Sn	−91	−62	−19	−3	−2	−16	−22	+10	−69	−8	−6	−21
Pb	−86	−44	+4	+22	+25	+8	+2	+41	−46	+4	+4	−3
Sb	−119	−83	−31	−9	−4	−16	−20	+3	−63	−8	−6	−13
Bi	−98	−55	−5	+15	+18	+2	−4	+33	−52	+1	+2	−4

3. Concluding remarks

In the present paper, it has been demonstrated that heats of formation can be calculated in a straightforward way, using the macroscopic atom model, for liquid alloys in general and for solid compounds containing a transition metal. For a third group of alloys, solid alloys of two non-transitional metals, the predictive power of the model is limited: only if one knows that an alloy is truly metallic can one give a reasonably accurate estimate of its heat of formation, otherwise the applicability of the model is limited to liquids. In this concluding section, we wish to comment on a few points relevant to the relation between liquid and solid alloys: size-mismatch energies in solid solutions, ordering tendencies in concentrated liquid alloys, coordination-number effects, and structural energies.

Thus far, we have avoided the discussion of solid solutions. There is an essential difference between solid and liquid solutions. In solid solutions, where atoms of different sizes have to occupy equivalent lattice positions, an additional positive contribution to the alloying energy arises, due to the elastic deformations necessary to accommodate the size mismatch. In liquids and solid compounds there is no such energy.

The size mismatch energy is the basis of the well-known Hume–Rothery rule for the occurrence of solid solutions in a binary system. The rule says that in order to have appreciable solid solubility, the atomic radii of the two constituents must not differ by more than 15%.

The size-mismatch energy can be estimated from the elastic constants and the relative size difference of the two metals, using Eshelby's elastic continuum theory [36]. Assuming, for simplicity, that Poisson's ratio is 0.3 for all metals, we can approximate Eshelby's result (for not too different metals) as

$$\Delta H_{\text{size}} = 1.25\, \overline{BV}_{\text{m}}\, \delta^2\, c_{\text{A}}\, c_{\text{B}}\,. \tag{19}$$

Here, $\overline{BV}_{\text{m}}$ is the average value of the product of bulk modulus and molar volume, and δ is the relative size difference defined as

$$\delta = 2\,(V_{\text{A}}^{1/3} - V_{\text{B}}^{1/3})/(V_{\text{A}}^{1/3} + V_{\text{B}}^{1/3}). \tag{20}$$

From the values of BV_{m} collected in table I, one can see that the size-mismatch energy becomes of the order of magnitude of the other terms considered here only for size differences exceeding 15%.

In the literature [37], a size-mismatch term has been introduced in the discussion of liquid alloys, where we feel an electron-density term is more appropriate. Such confusion can easily arise, because, due to the correlation between n_{ws} and V_{m}, in alloys for which the density mismatch, $n_{\text{ws}}^{1/3}$, is large, there is a large difference in the size of atoms too. However, it can be demonstrated with reference to exceptions that the two descriptions are not equivalent, and the distinctive feature of liquid alloys with large positive heats of mixing is a difference in n_{ws}. This is convincingly illustrated by the large positive ΔH_{mix} of alloys like Cu–Fe, Ag–Rh, Ag–Ru, etc., where there is no difference in the molar volumes of the constituents, but a large difference in the corresponding n_{ws} values (see table I).

In their recent analysis of heats of mixing of liquid alloys, Boom et al. [15] noticed that if the predicted value for the integral heat of mixing at the equiatomic composition gets below −20 kJ/mole, the experimental values tend to be clearly more negative than the predicted ones. Such a difference did not occur in the corresponding heats of solution. The reason for this discrepancy is short-range ordering in the liquid alloy that will take place if $\Delta H < -RT$. The energy of the alloy can be lowered by an amount corresponding to the difference in $f(c^{\text{s}})$ for ordered and disordered compositions.

We have indicated, as a special type of energy contribution related to crystal structure, the coordination-number effects, being responsible for the stability of compounds like KZn_{13}. Comparable compositions exist among transition metal compounds as well (e.g., YBe_{13}, $LaZn_{11}$, U_2Zn_{17}, etc.). Comparing experimental and calculated ΔH values for this type of compounds [14], we can estimate the order of magnitude of the coordination-number energies. Generally, they are of the order of −5 kJ/mole; only for compounds of Be this value is exceeded substantially. In atomic terms, a coordination-number energy can be understood by considering the shape of the atomic Wigner–Seitz cells. In a cell model the energy of a metal atom in first approximation depends only on the cell volume. In second order, however, the shape of the cell enters, the energy being the lower, the more the

Wigner–Seitz cell approaches a sphere. As a high coordination number means a more spherical Wigner–Seitz cell, this is seen as the source of the coordination-number energy.

In alloys of transition metals, structure-dependent energy terms do not significantly contribute to the heat of formation of the stable phases in a binary system. As explained before, this implies that the energy lowering achieved by giving the phase the crystal structure it has got, is about the weighted average of the heats of fusion of the two constituent metals. One must realize that this cancellation of structure-dependent terms holds for the phases that exist in equilibrium; nothing is said about the many other metastable phases one might think of. Evidently, for other phases than the equilibrium one, (phases for which the relative sizes of the two atoms are not suitable, a b.c.c. metal in an f.c.c. intermediate phase, etc.), there is a deviation from the calculated ΔH values in the positive direction.

Some insight is gained in this complicated matter by studying the relation between the average number of stable intermediate phases in a binary system and the (calculated) extreme values of the integral heat of formation. A histogram that summarizes phase diagram information on binary alloys of two transition metals is reproduced in fig. 24. If the heat of formation at the equiatomic composition is large and negative, $\Delta H < -75$ kJ/mole, the average number of intermediate phases is 5. With less negative ΔH, the number decreases, and at the other extreme, for $-4 > \Delta H > -10$ kJ/mole, there is only one intermediate phase. The histogram can be used to construct a schematic diagram of the average enthalpy differences, on a realistic scale, found between the first, most favoured crystal structure-composition combinations, and a number of additional, next-preferred ones.

The situation sketched in fig. 25 represents the experimental information on the average number of intermediate phases existing in a given ΔH interval. The picture implies that there is a limited number of competing structure-composition combinations within an enthalpy difference of 5 kJ/mole from the most favourable phase. There will be a lot of them at energy differences between 5 and 10 kJ/mole, and there can be many more at energies around 10 kJ/mole above the most stable phase. This order of magnitude of the structure-dependent energy contributions

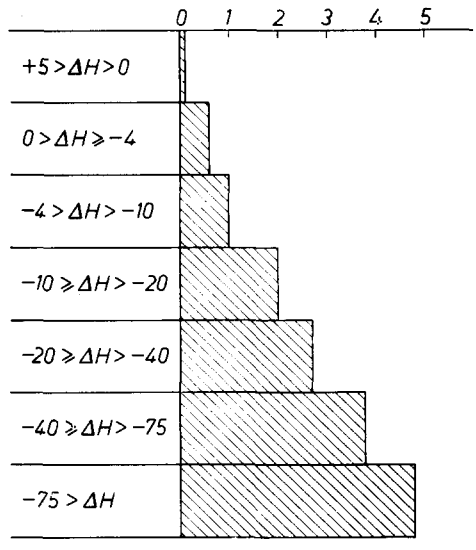

Fig. 24. The relation between the number of stable intermediate phases in a binary system and the value of the enthalpy of formation at the 50/50 composition. The histogram summarizes the experimental phase diagram information for combinations of two transition metals.

is very reasonable, being a fraction of the heat of fusion of transition metals, which range between 15 and 35 kJ/mole (see fig. 16).

Before we discuss the accuracy of our formation-enthalpy estimates, a few remarks have to be made concerning the different forms of the density-mismatch term. In section 1.4 we have introduced this term in the form of relation (4): $\Delta H \sim (\Delta n_{ws}^{1/3})^2$. However, in further calculations and in the determination of the ratio Q/P from the analysis of the sign of ΔH, th form of relation (7),

$$\Delta H_{sol} \sim 2V_B^{2/3} (\Delta n_{ws}^{1/3})^2 / [n_{ws}^{A})^{-1/3} + (n_{ws}^{B})^{-1/3}],$$

has been used. For small differences of n_{ws}, the expressions are equivalent; they will differ by a factor 4/9. One may ask to what extent differences in n_{ws} are still small for realistic alloy systems. The question is answered in fig. 26: at differences in $n_{ws}^{1/3}$ as large as a factor of two, the two relations are still equivalent. Checking table I, one will find that among transition metals the largest difference in $n_{ws}^{1/3}$ that occurs amounts to a factor 1.7 (Re–La). The only difficulties we may encounter are with alloys of the low melting

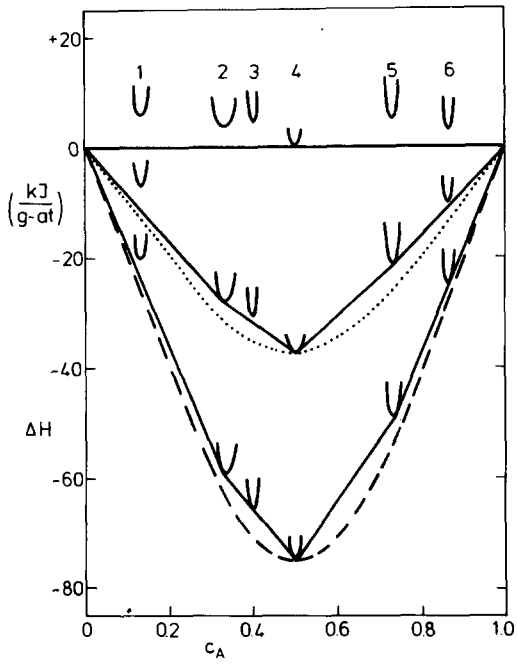

Fig. 25. An imaginary set of intermediate phases that reproduces the phase diagram information of fig. 24 at $T = 0$. If the extreme value of $\Delta H = 0$ the most favourable combination of composition and crystal structure (here phase 4) is just stable. If ΔH for the 50/50 composition equals -37 kJ/mole there are three stable phases 2, 4 and 5. For $\Delta H < -75$ kJ/mole five phases become stable, keeping the energy differences of the phases the same relative to the curve that represents the structure independent contributions to ΔH. The only phase that is not stable here is phase 1; of this type there may be many more that have been omitted. The drawing is schematic and arbitrary. Still, it serves to indicate the order of magnitude of the energy differences among the more favourable crystal structures in the average case. It is an artifact of the presentation that for the curve with $\Delta H_{50/50} = -75$ kJ/mole the stable phases tend to have heats of formation values above that of the dashed curve representing relation (9). In practice the empirical constant P will have got a somewhat smaller value, so that the dashed curve does not deviate systematically from the drawn one.

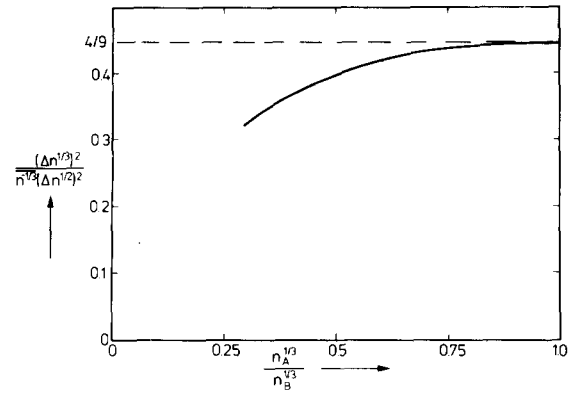

Fig. 26. The positive term in the heat of formation is used in the form $(\Delta n^{1/3})^2(n_A^{-1/3} + n_B^{-1/3})$ whereas in section 1.3 we have derived it as $(\Delta n_{WS}^{1/2})^2$. It is shown there that for difference in $n_{WS}^{1/3}$ up to a factor 2, the difference between the two forms can be neglected.

point alkali metals, Cs, Rb, and K with the high melting point transition metals. However, these do not have to be considered proper alloy systems: the predicted heats of formation are positive and extremely large (350 kJ/mole for the heat of solution of W in Cs).

It is not possible to assess in general terms the accuracy of the predicted ΔH values as given in tables II, III and V and in more complete form in subsequent papers. The accuracy will depend on the type of system (order of magnitude of ΔH, region of the periodic table, etc.) one is considering. For some metals (e.g. Hg) the results are systematically less satisfactory than for others. If one is interested in a predicted value for a system for which there is no experimental information, much can be learnt about the accuracy from a comparison of prediction and experiment for somewhat related systems. Such a comparison requires an as complete as possible collection of experimental data on heats of formation and a simultaneous consideration of all kinds of interfacial energy effects.

To provide such a survey is the purpose of the present series of articles.

In the next paper in the series, liquid and solid alloys of Sc, Ti and V will be discussed, and all available relevant experimental information on these systems will be summarized. The series will be continued with the other 3d metals, and as more and more materials are covered, the accuracy of our method will be easily judged. A wide range of problems, including such seemingly unrelated phenomena as surface segregation, the stability of hydrides, intermetallic molecules, heats of adsorption, and the surface tension of liquid alloys, will be touched upon in connection with materials for which these are relevant, either from the practical or the fundamental point of view (see also ref. 38). The interplay of practical and fundamental

considerations will characterize the whole series in that our primary purpose is to provide practically useful data, but, being aware of the limited nature of this approach, we permanently seek connections with alternative and more fundamental treatments.

References

[1] Rare Gas Solids, M. L. Klein and J. A. Venables, eds., (Academic Press, New York, 1976).
[2] F. Herman and S. Skilman, Atomic Structure Calculations (Prentice Hall, Englewood Cliffs, 1963).
[3] V. L. Moruzzi, A. R. Williams and J. F. Janak, Phys. Rev. B10 (1974) 4856.
[4] P. Hohenberg and W. Kohn, Phys. Rev. 136 (1964) B864.
[5] A. R. Miedema and R. Boom, Z. Metallkde 69 (1978) 183.
[6] A. R. Miedema, Z. Metallkde 69 (1978) 287.
[7] G. Lang in Handbook of Chemistry and Physics, 57th edition (1977).
[8] J. A. Alonso and L. A. Girifalco, J. Phys. F: Metal. Phys. 8 (1978) 2455.
[9] A. R. Williams, paper presented at Symposium Theory of Alloy Phase Formation, American Metallurgical Society Meeting, 1979, New Orleans.
[10] A. R. Miedema, F. R. de Boer and P. F. de Châtel, J. Phys. F: Metal. Phys. 3 (1973) 1558.
[11] J. H. Hildebrand and R. L. Scott, The Solubility of Non-Electrolytes (Reinhold, New York, 1956).
[12] J. Langmuir, edited in chap. IX of ref. 11.
[13] A. R. Miedema, R. Boom and F. R. de Boer, J. Less-Common Met. 41 (1975) 283.
[14] A. R. Miedema, J. Less-Common Met. 46 (1976) 67.
[15] R. Boom, F. R. de Boer and A. R. Miedema, J. Less-Common Met. 45 (1976) 237; 46 (1976) 271.
[16] B. W. Mott, Phil. Mag. 2 (1957) 259; J. Mat. Sci. 3 (1968) 424.
[17] L. Pauling, The Nature of the Chemical Bond, Cornell Univ. Press, Ithaca, 1960.
[18] B. P. Burylev and V. V. Vasilev, Russian J. Phys. Chem. 43 (1969) 1556.
[19] I. T. Sryvalin, O. Esin and V. G. Korpachev, Russian J. Phys. Chem. 40 (1966) 965.
[20] R. Kumar, J. Mat. Sci. 7 (1972) 1409, 1426.
[21] A. R. Miedema, J. Less-Common Met. 32 (1973) 117.
[22] W. H. Skelton, N. J. Magnani and J. F. Smith, Met. Trans. 1 (1970) 1833; 2 (1971) 473.
[23] R. Hultgren, P. D. Desai, D. T. Hawkins, M. Gleiser and K. K. Kelley, Selected Values of the Thermodynamic Properties of Metals and Alloys, Am. Soc. Metals, Ohio, 1973.
[24] J. A. Alonso and L. A. Girifalco, J. Phys. Chem. Sol. 39 (1978) 79.
[25] J. J. van den Broek, Phys. Letters 40A (1972) 219.
[26] K. A. Gschneidner, Solid State Physics 16, F. Seitz and D. Turnbull, eds., (Academic Press, New York, 1964) p. 275.
[27] W. B. Pearson, Handbook of Lattice Spacings and Structures of Metals (Pergamon Press, Oxford, 1967) Vol. 2.
[28] L. Brewer and P. R. Wengert, Met. Trans. 4 (1973) 83.
[29] M. Hansen and K. Anderko, Constitution of Binary Alloys (McGraw-Hill, New York, Toronto, London, 1958) and supplements by R. P. Elliot (1965) and F. A. Shunk (1968).
[30] R. Thümmel and W. Klem, Z. Anorg. Allg. Chem. 376 (1970) 44.
[31] M. Gambino and J. P. Bros, Thermochim. Acta 6 (1973) 129.
[32] G. Bruzzone, Acta Cryst. B27 (1971) 862.
[33] N. B. Hannay, Semiconductors (Reinhold, New York, 1959).
[34] R. Gobrecht, Phys. Stat. Sol. 13 (1966) 424, Ann. Phys. 20 (1967) 262.
[35] P. C. P. Bouten and A. R. Miedema, J. Less-Common Met. 65 (1979) 217.
[36] D. J. Eshelby, Solid State Physics 3, F. Seitz and D. Turnbull, eds. (Academic Press, New York, 1956) p. 79.
[37] B. Predel and H. Sandig, Z. Metallkde 56 (1965) 791; 60 (1969) 208.
[38] A. R. Miedema and P. F. de Châtel, Proc. Symposium Theory of Alloy Phase Formation, New Orleans 1979, L. D. Bennett, ed. (Amer. Soc. for Metals).